

## Simulations of a Satellite System for Co-Location in Space

*Master of Science Thesis in the Master Degree Programme, Radio and Space Sciences*

**Syed Zohaib Ali**

Department of Earth and Space Sciences  
Space Geodesy and Geodynamics Research Group  
CHALMERS UNIVERSITY OF TECHNOLOGY  
Göteborg, Sweden, 2013  
Report No. xxxx

# Table of Contents

Abstract .....	ii
Acknowledgments.....	iii
1 Introduction.....	1
1.1 GRASP overview and mission description .....	1
1.2 Innovative instruments on GRASP .....	1
1.3 Important science goals to achieve.....	1
2 Coordinate Systems .....	4
2.1 Earth Centered Inertial (ECI) .....	4
2.2 Earth Centered Earth Fixed (ECEF).....	5
2.3 Topocentric Coordinate System .....	5
2.4 Coordinate transformation.....	6
3 Two Line Element Sets (TLEs) .....	10
4 Simplified Perturbation Models.....	16
4.1 SGP.....	16
4.2 SGP4.....	16
4.3 SDP4.....	17
4.4 SGP8.....	17
4.5 SDP8.....	17
5 The visibility of GPS satellites as seen from a co-location satellite.....	19
5.1 Condition for visibility .....	19
6 Least-Squares Estimation using GPS .....	22
7 Results and Discussions.....	27
8 Light-Time Equation.....	35
9 Geometric Dilution of Precision (GDOP) .....	36
10 VLBI for spacecraft tracking .....	38
10.1 Principle of VLBI observation.....	38
10.2 VLBI delay model .....	39
11 Coordinates determination by VLBI.....	40
11.1 VLBI delay in terms of Light-time equation.....	41
11.2 Least-Squares Estimation for VLBI.....	42
11.3 Determination of the a-priori satellite position .....	44
12 Results & Discussion .....	47
13 Conclusion .....	63
References.....	64

# Abstract

This thesis work investigates the potential performance of the future co-location satellite mission, GRASP, by presenting the simulations in the MatLab environment. The purpose of GRASP is to assess the potential performance of geodetic techniques combined in space. One of the satellites, acting as a GRASP, of different satellite constellations; like Globalstar, Iridium and Orbcomm, was tested for different orbital height, inclination, eccentricity etc. LAGEOS-1 satellite was also tested for the higher altitude of 6000 km. NORAD's (North American Aerospace Defense Command) TLEs (Two-Line Element Sets), containing the mean orbital elements, were used to generate orbital state vectors of position and velocity for the selected satellites by performing orbit propagation with the SGP4 (Simplified Perturbation Models) as implemented in 'Revisiting Spacetrack Report #3'. The Globalstar, Iridium, Orbcomm and LAGEOS-1 satellites were selected as the co-location satellite and their coordinates were determined by the GPS constellation and also by the VLBI network of ground stations. One day orbital data with time steps of 1 minute and 1 second were generated by the SGP4 propagator and passed to the MatLab code for coordinate determination by GPS and VLBI respectively. The 30 GPS satellites were taken from the GPS constellation for higher visibility of the co-location satellite. A VLBI network of 21 existing stations was chosen such that it is spread throughout the globe to provide maximum visibility and improved coordinate determination for co-location satellite.

# Acknowledgments

This thesis report is submitted to the Department of Earth and Space Sciences in partial fulfillment of the requirements of the degree of Master of Science in Radio and Space Sciences at Chalmers University of Technology, Sweden. The work was carried out in the Space Geodesy and Geodynamics research group, Department of Earth and Space Sciences, Chalmers University of Technology, under the supervision of Associate Professor Rüdiger Haas, Head of Space Geodesy and Geodynamics research group, Department of Earth and Space Sciences, Chalmers University of Technology, Sweden.

First of all I would like to thank Almighty ALLAH, the most merciful and beneficent, for giving me strength to carry out this project work.

I would like to thank my supervisor, Associate Professor Rüdiger Haas for assigning me thesis work according to my interests and providing support and motivation throughout the project. He was always nice, calm and friendly. I never saw such a friendly teacher in my whole academic life. Also my sincere gratitude for providing me with the laptop for thesis work, this is one of many examples that he was abundantly helpful in several ways. The discussions I had with him are invaluable.

Last but not least, I would like to thank my father, my brother and my sisters for their support, prayers and love throughout my studies. Thanks to my dear father for providing me everything from childhood to this stage. I want to tell him that I got inspirations from you to become a telecommunication engineer. When I entered into world of telecoms, I worked on establishing microwave line-of-sight links, and this work injected in me a desire to do MS in satellites and space related fields. My sincere prayers for my deceased mother she is not with me but her prayers are always. Thanks to my dear brother, Imran, for supporting me financially and being truly brother when needed. Thanks to my both sisters, Shazia and Sabeen, for pushing father to send me for higher studies and praying all the time for my success. All my successes to this stage are because of both of you. What I have achieved so far, it is just for all of you. Thanks!

Syed Zohaib Ali



# 1 Introduction

## 1.1 GRASP overview and mission description

The Geodetic Reference Antenna in Space (GRASP) is a proposed micro-satellite mission concept devoted to the improvement of all the geodetic techniques like GNSS, VLBI, SLR, and DORIS. It was proposed to NASA in September 2011 and is expected to launch in early 2016 for the duration of 3 years. The GRASP spacecraft consists of four geodetic sensors devising it a space-based co-location science instrument [1]. The Terrestrial Reference Frames (TRF) and Celestial Reference Frames (CRF) are established and maintained by these space geodetic techniques. All these techniques have their own strengths and weaknesses and are used together to complement each other. A co-location system is a best way to nullify their weaknesses. The advantages and disadvantages of an individual technique make it vulnerable to be used for the variety of geodetic observations. A co-location system will have the ability to send artificial VLBI signals, receive GNSS and DORIS signals and reflect SLR signals opening new horizons for understanding the Earth and Space by improving the CRF and specially TRF [26].

## 1.2 Innovative instruments on GRASP

GRASP is a standalone geodetic science instrument in space carrying all the four space geodetic sensors to constitute a co-location system. The geodetic sensors includes: Global Navigation Satellite System (GNSS), Very Long Baseline Interferometry (VLBI), Satellite Laser Ranging (SLR), Doppler Orbitography and Radio-positioning Integrated on Satellite (DORIS). A short description about each of these techniques is given in the following section.

## 1.3 Important science goals to achieve

The immense and far-reaching science goals to achieve from a functional GRASP mission include [1]:

- Mission will find relationships between several geodetic techniques in an agreeable reference frame.
- The data obtained by the observation in existing geodetic techniques form the basis of TRF. An optimal TRF realization requires joint processing of data from several techniques. GRASP will implement the joint processing of data for this purpose.
- GRASP will increase the precision for all precise GNSS, DORIS, SLR and VLBI applications.
- Many science missions like OSTM, ICESAT-II, SWOT, DesDynI, GRACE-II etc., depends on GNSS for precise science measurements. GRASP will improve the accuracy for these missions.
- GRASP will facilitate the adjustment and constant data processing from the growing diversity of GNSS.
- GRASP will provide steady measurements of sea surface height, ice elevations, gravity field variations etc.

Terrestrial frames are developed through the analysis of data from Earth-orbiting satellites.

There are various geodetic satellites orbiting the Earth which sends observed data to the ground tracking stations. The terrestrial frames are developed by the analysis of these observed data [2]. Every geodetic technique inherently produces more accurate measurements in their natural reference frames that have unique advantages and disadvantages concerning the geodetic technique so frame interconnections are necessary to take advantage of the unique contributions of various geodetic techniques. This can be achieved by a co-location satellite system that can combine all existing geodetic techniques into a single satellite [1].

A short introduction of geodetic techniques implemented on GRASP, is presented below. GNSS and VLBI are discussed in detailed in Part 1 and Part 2, respectively, as they are the primary techniques used in this project work.

**DORIS:** Doppler Orbitography and Radio-positioning Integrated by Satellite, a French satellite system, is used for the orbit determination of satellites and positioning of the ground stations. In this system the satellite receives signals, emitted by beacons installed on the ground, and sends back to the ground which is slightly changed in frequency by the Doppler Effect. It is included as a host research project on several space missions like Spot-2, -3, -4, -5, Topex/Poseidon, Jason, ENVISAT and CryoSat [3].

**SLR:** Satellite Laser Ranging is a ranging system that uses ultrashort laser pulse to locate the satellites. Satellites equipped with retro-reflectors, reflects the laser signals back to the Earth station. The measurement of round trip time of flight of the laser signal gives a millimeter level precised range measurements for the satellite. These range measurements provide range data for accurate orbit determination and science products for other host technologies.

**GNSS:** Global Navigation Satellite System is a navigation system used to determine the geographic position of an object located anywhere on the surface of the Earth. It determines the geographic location by the help of triangulation that require three satellites in view of the receiver for its geographic position determination. A fourth satellite is also needed to minimize the timing error and a more accurate position determination. GPS (Global Positioning System), GLONASS, GALLILEO, COMPASS etc., are various GNSS techniques existing today, but the GPS has been used in this project work because of its dense network of satellites and is widely used by civilians all around the world. Apart from position determination, GNSS can also be used for various geodetic applications like weather prediction, estimation of tectonic plate motion etc. A detailed description of how the GPS can be used for spacecraft position determination is discussed in Chapters 5 and 6.

**VLBI:** VLBI (Very Long Base Line Interferometry) is an interferometric technique developed for radio astronomy with the purpose to improve the angular resolution. It is an astronomical interferometer that consists of two or more telescopes, relatively at very large distances of several thousands of kilometers, combined together to present a telescope of the same diameter as the distance between them, thus improving the angular resolution of the system. The VLBI technique was primarily developed for the observation of extragalactic radio sources such as Quasars but nowadays it is also been widely used for the observation and tracking of near-Earth and deep-space spacecraft. A detailed description about principle of VLBI observation and how it is used for spacecraft tracking is discussed in Chapter 10.

As there is no existing co-location satellite, so some existing Earth orbiting satellites were chosen in this project to be used as a co-location satellite. The chosen satellites are given in the Table 1 with their orbital information and names in all three formats.

Table 1: satellite's names and orbital information

NORAD id	Int'l code	Name	Period (minutes)	Inclination (degrees)	Perigee (km)	Apogee (km)	Eccentricity
37744	2011-033F	GLOBALSTAR M089	114.1	52.0	1,420.2	1,421.3	0.0000607
24795	1997-020D	IRIDIUM 5	100.4	86.4	782.8	786.9	0.0002194
25986	1999-065G	ORBCOMM FM 34	100.7	45.0	795.5	802.9	0.0003941
8820	1976-039A	LAGEOS 1	225.5	109.8	5,844.8	5,955.6	0.0045068

The eccentricity given in Table 1 is taken from the TLEs of respective satellites at a particular epoch. The other information is taken from the website [www.n2yo.com](http://www.n2yo.com). At other epochs there might be a slight change in the eccentricity due to perturbation effects that can be neglected. A TLE (Two-Line Element Set) is a format of two lines of 69 characters each and contains mean orbital elements of the satellite that describes the orbit of the satellite. The TLEs, for each of the satellites, used in this project are given below in Table 2.

Table 2: TLE (Two-Line Element Set) of selected satellites

Sr. no.	TLE (Two-Line Element Set)
1	37744 1 37744U 11033F 12058.78499768 -.00000086 00000-0 10000-3 0 2034 2 37744 51.9918 214.5920 0000607 111.9935 248.0987 12.62268085 31388
2	24795 1 24795U 97020D 12208.44591533 .00000196 00000-0 63036-4 0 1666 2 24795 86.3973 345.7566 0002194 59.6702 300.4729 14.34220345797181
3	25986 1 25986U 99065G 12208.57542827 .00000430 00000-0 21960-3 0 4456 2 25986 45.0419 255.4887 0003941 299.0451 61.0004 14.29832474659703
4	08820 1 08820U 76039A 12207.58044721 .00000020 00000-0 10000-3 0 3233 2 08820 109.8341 240.9978 0045068 308.7224 50.9547 6.38664782589488

The detailed description about TLE is given in Chapter 3.

## 2 Coordinate Systems

A coordinate system is defined by specifying its origin, a fundamental plane and the preferred direction [4]. There are many coordinate systems that are used in satellite orbit determination and satellite geodesy. The coordinate systems that are used in this project are described here.

### 2.1 Earth Centered Inertial (ECI)

The most common system in astrodynamics is the Earth Centered Inertial (ECI) system. It's a non-rotating coordinate system centered at the center of mass of the earth. Non-rotating means, it does not move with the rotation of the Earth to keep itself fixed with respect to the Earth rather it remains fixed and the Earth rotates beneath it. The fundamental plane for the ECI system is the Earth's equatorial plane. The x-axis points in the principal direction of the vernal equinox, the y-axis points 90 degrees to the East and the z-axis passes through the North Pole.

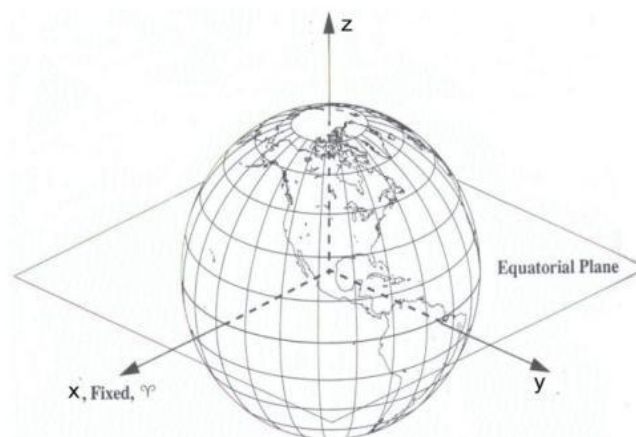


Figure 1: The Earth-Centered Inertial Coordinate System. [5]

The orbital motion of an object in space is defined by equations of motion which are very convenient to describe in non-rotating ECI frame as compared to rotating coordinate systems. That is why SGP4 utilizes the ECI frame to generate the position and velocity vectors of a satellite in orbit. SGP4 is an extension of SGP (Simplified General Perturbation) model, an orbit propagator that generates realistic orbital path of the satellites by propagating TLEs (Two-line element sets), generated by NORAD (North American Aerospace Defense Command), forward in time. The detailed description about TLE is presented in Chapter 3 and the detailed description about SGP4 is presented in chapter 4. The ECI frame is also very convenient to indicate directions towards other celestial bodies.

## 2.2 Earth Centered Earth Fixed (ECEF)

The Earth Centered Earth Fixed (ECEF) coordinate system is a rotating coordinate system that is rotating with the Earth. It is unlike the ECI system that is non-rotating with the Earth. The ECEF system is centered at the center of the Earth with the principal axis pointing towards the intersection of the prime meridian with the equator.

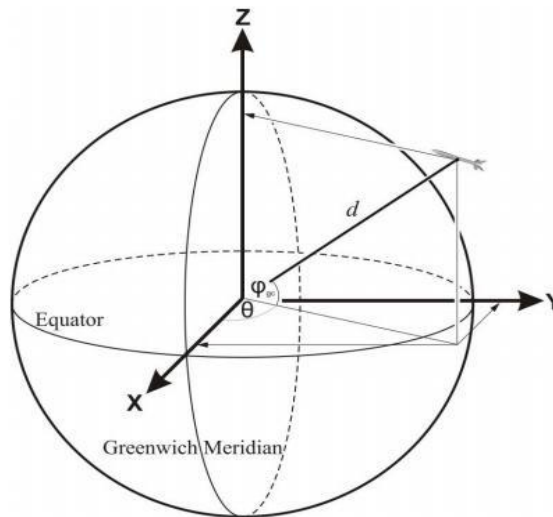


Figure 2: The Earth Centered Earth Fixed Coordinate System. [5]

## 2.3 Topocentric Coordinate System

In the topocentric coordinate system the observer or a receiver is at the origin of the system. The fundamental plane is the local horizon, that is, a tangent to the surface of the observer on the Earth. The location of an object in this system is defined by two angles, Azimuth and Elevation. Azimuth is the angle that is measured eastward from the North to the object meridian. Elevation is the angle measured positively upward from the observer's local horizon to line of sight of the object. The distance measured from the observer to the object is called the Range [24].

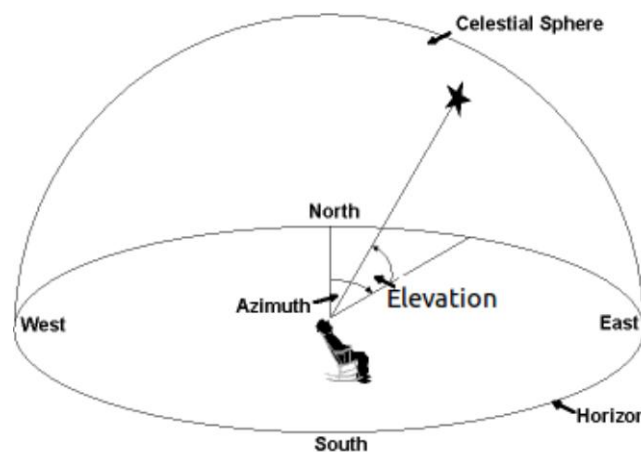


Figure 3: The Topocentric Coordinate System. [25]

## 2.4 Coordinate transformation

The orbital state vectors generated by the SGP4 are in the ECI coordinate system. Terrestrial objects are more conveniently represented in the ECEF coordinate systems. The ground tracks of satellites, projected on the Earth's map, are plotted in ECEF system after conversion from the ECI system. As an example, Figure 4 depicts the ground track of Globalstar satellite plotted in the ECEF system for a period of one day.

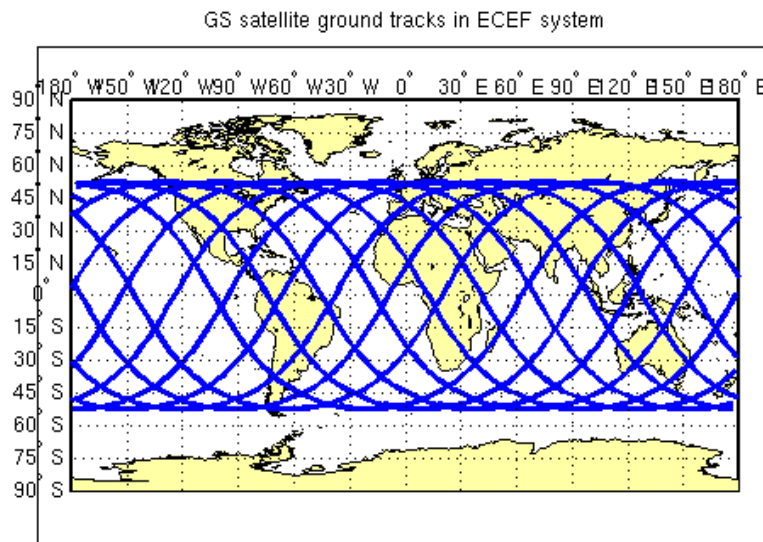


Figure 4: Groundtrack of Globalstar satellite plotted in ECEF system.  
(Plotted for one day)

An important point to be noted here is that the satellite's orbit are more easily interpreted as circular or elliptical when plotted in the ECI system. To illustrate the difference between the orbits presented in ECI and ECEF frames, Figures 5 and 6 are given below:

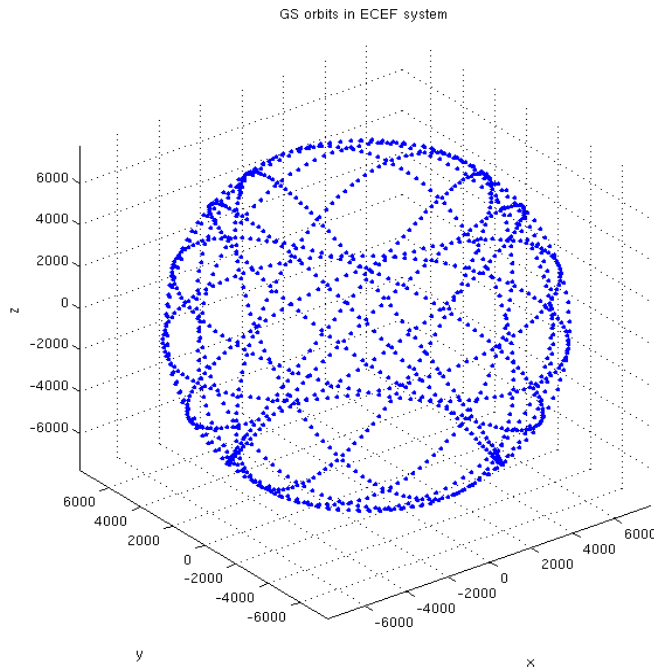


Figure 5: Globalstar orbit in the ECEF system.

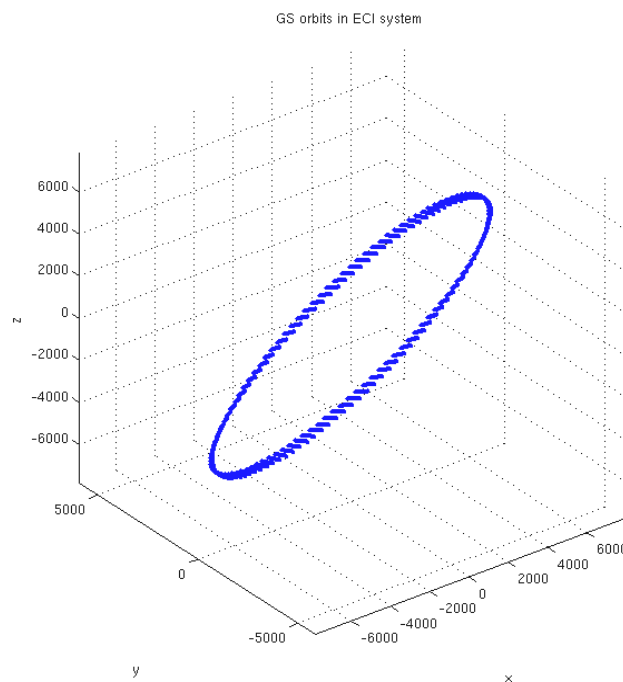


Figure 6: Globalstar orbit in the ECI system.

The orbital period of the Globalstar satellite is 114.1 minutes, so the satellite completes 12.6 revolutions per day. In the figures above, the satellite's orbits are plotted for duration of one day so there are 12.6 orbits in each figure. These orbital passes are generated by the SGP4 propagator that includes the perturbations effects on the satellite like earth's gravity and atmospheric drag. This perturbation effect is more clearly viewed in Figure 6 where the plotted points do not overlap on each revolution. If the perturbation effects are excluded the points should coincide on each revolution.

Form Figures 5 and 6, it becomes clear that the Globalstar orbit is more clearly seen as circular in

the ECI system. Satellite observations from a site are done in the ECEF system which is more useful than in the ECI system, so the orbital state vectors in the ECI system generated by SGP4 are converted to the ECEF system before doing further calculations. The orbital state vectors generated by the SGP4 consists of both the position and velocity vectors but only the position vectors are used in this project to determine the satellite coordinates by GNSS and VLBI. So the transformation method for the position vectors is described below.

The transformation of the position vector from the ECI to the ECEF system can be achieved by using the following matrix equation [6]:

$$\mathbf{r}_{ecf} = [\mathbf{T}] \mathbf{r}_{eci} \quad (2-1)$$

where T is the transformation matrix and is given by [6]

$$A = \begin{bmatrix} \cos \theta & \sin \theta & 0 \\ -\sin \theta & \cos \theta & 0 \\ 0 & 0 & 1 \end{bmatrix} \quad (2-2)$$

Here  $\theta$  denotes the Greenwich sidereal time at a specific epoch which is given by [6]

$$\theta = \theta_{g0} + \omega_e t \quad (2-3)$$

here  $\theta_{g0}$  indicates the Greenwich sidereal time at 00:00:00 UT,  $\omega_e$  denotes the inertial rotation rate of the Earth, and  $t$  is the time duration since 0 hours UT [6].

The Globalstar satellite travels West to East in the same direction as the Earth rotation. There are also many satellites that travel in the opposite direction i.e. from East to West. So the orbits can be divided in two categories, prograde and retrograde, depending on the direction of motion of satellite. These categories are defined below:

**Prograde orbit:** A satellite having an orbital inclination of less than  $90^\circ$  and travels in the same direction as the rotation of Earth around its own axis i.e. from West to East direction, this orbit is called a Prograde orbit.

This can be explained by Figure 7 on next page.

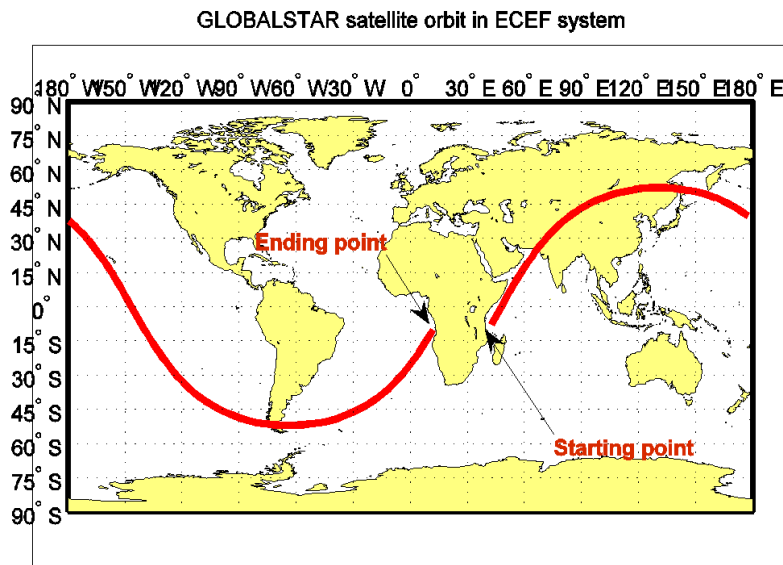


Figure 7: Illustration of a prograde orbit

This figure illustrates the prograde orbit of the GLOBALSTAR satellite having an inclination of  $52^\circ$  which is less than  $90^\circ$ .

**Retrograde orbit:** A satellite having an orbital inclination of greater than  $90^\circ$  and travels in the opposite direction as the rotation of Earth i.e. from East to West direction, the orbit is called a retrograde orbit.

The figure below illustrates the retrograde orbit.

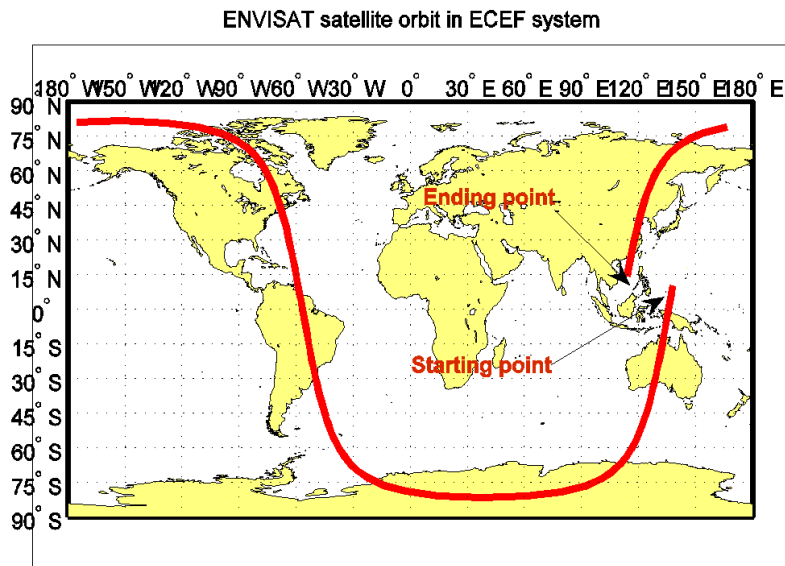


Figure 8: Illustration of a retrograde orbit

## 3 Two Line Element Sets (TLEs)

Six orbital elements are used to describe the orbit of an Earth's satellite and its orientation in space. A Two Line Element (TLE) set is a format that is used to describe the position of a satellite at a particular instant of time. This format consists of two lines of 69 characters of data containing the mean orbital element that is why it is called 'Two line Element sets'. The two TLE lines are usually followed by a title line that contains the satellite's name. This format is specified by the NORAD (North American Aerospace Defense Command) which is also responsible for generating and maintaining TLEs of thousands of Earth orbiting satellites and space debris. The satellite in its orbit is perturbed by many forces like atmospheric drag, Earth oblateness and lunar-solar perturbations. These perturbations change the shape and orientation of the orbit. The NORAD TLEs consists of mean orbital elements that average out these perturbation effects in a specific manner [20]. The right ascension and declination data of a satellite is taken, by observing the satellite by an optical or radio telescope, by SLR technique or other advanced observing techniques, for a short time period. These data is then passed through computer software that generates mean orbital element sets and other necessary parameters needed for the TLEs.

Satellite motion described by these mean orbital elements can be applied to orbit propagation softwares for predicting the trajectory of the satellite. The important point to be noted here is that during orbit estimation the orbit propagator must include the perturbing effects in the same manner as were excluded during the TLE generation otherwise the erroneous estimations will be achieved [7].

A TLE example for the International Space Station (ISS) is shown below:

```
ISS (ZARYA)
1 25544U 98067A 12069.11980714 .00018689 00000-0 24053-3 0 1541
2 25544 51.6413 263.8320 0017773 135.4419 323.7930 15.58923824762412
```

The description of the lines is as follows:

Line 1

Table 3: TLE Line 1 Format Definition [8]

Column	Description
01	Line Number of Element Data
03-07	Satellite Number
08	Classification
10-11	International Designator (Last two digits of launch year)
12-14	International Designator (Launch number of the year)
15-17	International Designator (Piece of launch)
19-20	Epoch Year (Last two digits of year)
21-32	Epoch (Day number and fractional portion of the day)
34-43	First Time Derivative of the Mean Motion divided by 2. or Ballistic Coefficient (Depending on ephemeris type)
45-52	Second Time Derivative of Mean Motion divided by 6. (Blank if N/A)
54-61	BSTAR drag term if SGP4 general perturbation theory was used. Otherwise, radiation pressure coefficient.
63	Ephemeris type
65-68	Element number
69	Check Sum (Modulo 10)

Line 2

Table 4: TLE Line 2 Format Definition [8]

Column	Description
01	Line Number of Element Data
03-07	Satellite Number
09-16	Inclination [Degrees]
18-25	Right Ascension of the Ascending Node [Degrees]
27-33	Eccentricity (decimal point assumed)
35-42	Argument of Perigee [Degrees]
44-51	Mean Anomaly [Degrees]
53-63	Mean Motion [Revs per day]
64-68	Revolution number at epoch [Revs]
69	Check Sum (Modulo 10)

The information from the above given example of TLE for 'ISS' can be extracted with the help of

Tables 3 and 4 as follows:

Line '0' is preserved for the satellite's Catalog Number or International ID. According to [17] there is a conflict in the choice of name's length which can be 11, 12 or 24 characters long depending on the requirements of some satellite propagation softwares. It can also be a Satellite's Common Name provided by some TLE distributors as an additional option for the propagating softwares. For the ISS TLE it is ISS (ZARYA).

Line 1 consists of 69 character spaces that start with the field of Line Number which denotes the line number of the line. For Line 0 the Line Number is not mentioned. First field of line 2 is also the line number.

The second field of line 1 and 2 are also same. These field represents the satellite's number that consists of characters 3 to 7.

Character 8<sup>th</sup> is the 3<sup>rd</sup> Field of line 1 named 'Classification'. It can be 'U' for unclassified data and 'C' for classified data. All the publicly available TLEs have 'U' for unclassified data.

Fields 4<sup>rd</sup>, 5<sup>th</sup>, and 6<sup>th</sup> of line 1 are reserved for the 'international designator' with characters 10 to 11 for last two digits of the launch year, characters 12 to 14 for launch number of the year and characters 15 to 17 for the piece of launch respectively.

For ISS the International designator is '98067A'. Here,

'98' is the Launch year

'067' is the 67<sup>th</sup> launch during the year 1998, and

'A' is the primary payload. Secondary payloads and launch vehicles are indicated by the subsequent letters like B, C, D, E, etc. [9].

The 7<sup>th</sup> and 8<sup>th</sup> fields of line 1 are reserved for the epoch at which the TLE was generated. Characters 19 to 20 shows the first two digits of the epoch year. Characters 21 to 32 shows epoch day and the fractional portion of the day. The month, day, hour, minute and seconds information can easily be extracted from these fields. The time is expressed in UTC format [9]. In the above TLE for ISS the Epoch is '12069.11980714', which can be expanded as:

Year=2012

Month=03

Day=09

Hour=02

Minute=52

Seconds=31.3369

Characters 34 to 43 represents the first time derivative of the mean motion divided by 2 in units of revolutions/day<sup>2</sup> and reserved for the field 9<sup>th</sup> while characters 45 to 52 represents the second time derivative of the mean motion divided by 6 in units of revolutions/day<sup>3</sup> and reserved for the 10<sup>th</sup> field. Both of these fields are utilized only by the simple SGP (Simplified General Perturbation) model but not by the SGP4/SDP4 model and provides no real scope [8]. SDP4 is an extension of SGP4 and it is described in Chapter 4.

Field 11 (characters 54-61) of line 1 represents the 'B-star drag' term.

$B^*$  (B-star) drag term is a SGP4 type drag coefficient that assess the atmospheric effects on the motion of satellites. It is calculated by the formula [9]

$$B^* = \frac{C_D \rho_o A}{2m} \quad (3-1)$$

where

$C_D$  = Drag coefficient

$\rho_o$  = Atmospheric density

$A$  = cross-sectional area of satellite

$m$  = mass of the satellite

$B^*$  is actually the adjusted value of  $B$ , Ballistic coefficient, by the atmospheric density  $\rho_o$ . According to aerodynamics theory, every object has a ballistic coefficient which is mathematically calculated by [8]:

$$B = \frac{C_D A}{m} \quad (3-2)$$

The ballistic coefficient shows the susceptibility of an object to the atmospheric drag, the higher the  $B$ , the more it is susceptible to the drag.

$B^*$  is an adjusted value of  $B$  using the reference value of atmospheric density,  $Q_o$  [8]

$$B^* = \frac{B \rho_o}{2} \quad (3-3)$$

Unit of  $B^*$  is (Earth Radii)<sup>-1</sup>.

The  $B^*$  term in the TLE of ISS is 24053-3 and it can be read as +0.24053e-3. A decimal point is assumed before the first digit and if there is no sign before the first digit, the + sign is assumed. The last digit is reserved for the exponent of base 10, positive if no sign before the last digit.

12<sup>th</sup> Field of line 1, character 63, is reserved for the 'Ephemeris type' that is the orbital model used to generate TLE data. The TLE Ephemeris Type is always set to zero for distributed data, although STR#3 suggests the following assignments: 1 = SGP, 2 = SGP4, 3 = SDP4, 4 = SGP8, 5 = SDP8 [7].

Field 13<sup>th</sup>, characters 65-68, is reserved for the 'Element Set Number' which represents the TLE count since the launch of the satellite. The Element Set Number of a specific satellite is incremented every time whenever a new TLE for that satellite is generated. This helps to keep track the order of the TLE for that satellite and to differentiate it from the other TLEs of same satellite. Practically sometimes it happens that the 'Element Set Numbers' does not get synchronized with the previous TLEs mainly due to switching of operation between the primary and the backup Space Control Centers. This makes hard to express whether we have all the elements sets for a designated satellite [8]. In the line 1 of above TLE, field 13<sup>th</sup> is 154<sup>th</sup> which represents the 154<sup>th</sup> TLE generated for the ISS since its launch.

The last character, 69, of line 1 and line 2 represents the checksum module. The purpose of this checksum character is to provide a simple error checking 'modulo-10' mechanism for the TLEs. According to [7], only a 90% detection rate is provided by the modulo-10 checksum for uniformly random errors. Also the values assigned to the characters are ambiguous, particularly the +sign is taken as 0. Having the checksum character, it is wise to look at other features in the TLE, such as compare the satellite number on each line, check the line numbers of each line as line one should start from '1' and line two from '2' etc. [7].

How the last character in both lines is calculated by the modulo-10 can be described, by considering

the line 1 of ISS's TLE given above, as follows:

- ⤴ Add all the numbers given in line 1.
- ⤴ Take letters, '.', 'and' '+' as "0".
- ⤴ Take '-' as "1".
- ⤴ the last digit of summation is the Checksum

here is the example:

1 25544U 98067A 12069.11980714 .00018689 00000-0 24053-3 0 1541

1+2+5+5+4+4+0+9+8+0+6+7+0+1+2+0+6+9+0+1+1+9+8+0+7+1+4+0+0+0+0+1+8+6+8+9+0+0+0+0+0+1+0+2+4+0+5+3+1+3+0+1+5+4 = 161

the last digit of the sum 161 is 1 which verifies the checksum modulo-10 of line 1.

## Line2

**2 25544 51.6413 263.8320 0017773 135.4419 323.7930 15.58923824762412**

Field 1 and 2 for line2 are the same as the line1 and have the same length in characters.

Field 3, characters 9 to16, denotes the inclination of the satellite orbit represented in degrees from 0 to 180. The inclination for the ISS in the given TLE is 51.6413°.

Field 4, characters 18-25, represents 'Right Ascension of the Ascending Node' (RAAN) also represented in degrees from 0 to 360. Satellite's ascending node precesses with time so an accurate epoch is required to express the time at which RAAN is valid [9]. The RAAN for the ISS in the above TLE is 263.8320° at the specified epoch of the TLE.

Character 27-33 are reserved for the 5<sup>th</sup> field and denote the eccentricity of the orbit. The decimal point for the eccentricity value is omitted in the TLE but it's assumed to be present there before the first digit of the eccentricity value. Eccentricity is always in the range of 0 to 1. The value 0 represents a circular orbit while 1 represents an elliptical orbit. The eccentricity for the ISS given in the above TLE is extracted as '0017773' and can be read as 0.0017773 representing an almost circular orbit.

6<sup>th</sup> field of line 2, Characters 35-42, represents the 'argument of perigee' expressed in degrees in the range between 0 to 360 degrees. For the ISS TLE it is 135.4419°.

Characters 44-51 are reserved for the 7<sup>th</sup> field of line 2 which is the 'Mean Anomaly'. It is also represented in degrees ranging from 0 to 360 degrees. The mean anomaly for the ISS in above TLE can be read as 323.7930 degrees.

'Mean Motion' is the 8<sup>th</sup> field of line 2 with characters 53-63. It is expressed in revolution per solar day. In the given TLE the value for the mean motion is '15.58923824' which is 15.58923824 revolutions per day.

The last field connected to line 2, preceding the checksum, is the revolution number. This field requires some clarification as there are various conventions for finding the revolution number. According to NORAD's convention, the revolution of a satellite within its orbit is the period between the consecutive ascending nodes that starts when the satellite reaches the ascending node. The important point to note here is that when a satellite is launched, the period from launch to the first ascending node is considered as revolution 0. The first revolution starts from the first ascending node. A satellite should reach the ascending node before its subsequent revolution number is calculated, this is due to the fact that most of the element sets are generated with epochs that spot the satellite close to its ascending node [8]. '76241' in the above TLE for ISS shows that the satellite has accomplished 76,241 orbits since its launch to the TLE generation epoch.

## 4 Simplified Perturbation Models

Satellite orbital parameters are calculated by the set of five mathematical models called SGP, SGP4, SDP4, SGP8 and SDP8 which are generally called Simplified General Perturbation models, SGPs. The Two-Line Element sets generated by NORAD, utilize SGP4 extensively due to which these set of five models are collectively referred to as SGP4 [10].

If the position and velocity of satellite or other space debris is known at a particular instant of time, SGP4 can be used to predict the future position of the satellite [11]. In reality the satellite's path is not ideal but it is changed by the perturbation forces like Earth's shape (spherical harmonics), atmospheric drag, radiation pressure, and gravitational effects from other bodies like the sun and the moon in general [12]. SGP4 keep track of these forces and generates a realistic orbital path of the satellite.

Satellites having orbital period less than 225 minutes are called Near-Earth satellites and SGP models are used to predict the trajectory of these objects. Similarly, satellites that have orbital period of greater than 225 minutes are called deep-space satellites and SDPs are used for the prediction of their orbital path [10]. By knowing the value of mean motion we can figure out if the satellite is near-earth or deep-space and use the appropriate SGP4 or SDP4 to generate TLEs and future predictions of satellite pass.

The variations of SGPs are briefly described below.

### 4.1 SGP

The first simplified perturbation model named SGP, used for near-Earth satellites, was formulated by Hilton & Kuhlman (1966) by simplifying the work of Kozai (1959) for its gravitational model. The motion of the satellite is affected by the gravitational drag and the mean motion is the averaged motion of the satellite over a prescribed duration of time. This model assumes the drag effect on mean motion as linear in time which defines a quadratic change of mean anomaly with time. The eccentricity of an orbit also changes due to the drag effects, which in turn affects the perigee and apogee height, but SGP models this effect in a way that preserves the constant perigee height [11].

### 4.2 SGP4

SGP4 is also used for near-earth satellites. It was formulated by Ken Cranford in 1970. In 1959 Brouwer presented a solution to the satellite theory without drag. In 1969 Lane and Cranford presented an improved drag theory for the satellites that used Brouwer theory for its gravitational model. Ken Cranford simplified this work further and produced SGP4 [11]. The SGP4 model generates an error of nearly 1 km at epoch and increases nearly 1 to 3 km per day [8].

### **4.3 SDP4**

The SDP4 model is a modification of the SGP4 model and is developed by Hujsak in 1979 to be used for the deep-space satellites. SDP4 use only simplified drag equations. Since the effects of atmospheric drags becomes lower as we go higher above the Earth's atmosphere or can be discarded for more deep-space orbits but the perturbations due to the sun and the moon becomes larger in effect so accounted in SDP4 model as Lunar-Solar perturbations. Earth resonance terms like sectoral and tesseral Earth harmonics are also included for geostationary and molnyia orbits [11]. The SDP4 model has an error of 10 km at epoch [10].

### **4.4 SGP8**

The SGP8 model is also used for near-Earth satellites. The extended analytical theory developed by Hoots used the models of gravitational and atmospheric effects that were developed by Lane and Cranford. The Hoots differentiated the differential equations in a very different style to simplify the work. The SGP8 model was obtained by simplifying the work of Hoots [11].

### **4.5 SDP8**

In the end, the extension of SGP8 model implemented for deep-space space satellites is SDP8 model. The equations used in SDP4 were also used in SDP8 to model the deep-space effects [11].

The 'Revisiting Spacetrack Report#3', by David Vallado, provides the MatLab code for SGPs where only the SGP4 and SDP4 are implemented. The reason is that the TLEs generated by the NORAD (North American Aerospace Defense Command) only utilize the SGP4 and SDP4. A simple condition is implemented in the code that checks for the satellite's orbital period. If the orbital period is greater than 225 minutes, SDP4 is selected. An important point to be noted here is that the TLEs should to be propagated by the same perturbation model that is used to generate them. Using other models will lead to the propagation full of errors unless we are agreeable to accept predictions with unpredictable errors [8].

## **Part 1**

# **Coordinate determination of a co-location satellite by GNSS**

This section describes a method implemented to estimate the co-location satellite's coordinates using the GNSS constellation. First, Chapter 5 discusses the condition implemented for calculate the visibility of co-location satellite as seen from a GPS constellation and derives the necessary equation with help of the Fig. 8. Chapter 6 explains the least-squares estimation process for coordinate determination with GPS measurements. The necessary equations are derived by considering Globalstar satellite as a co-location satellite. Chapter 7 presents the results and discussions.

## 5 The visibility of GPS satellites as seen from a co-location satellite

The aim is to simulate GPS measurements on a co-location satellite. These measurements shall be used in an analysis and the position of the co-location satellite shall be determined. To simulate GPS measurements, we need to know which and how many GPS satellites are visible for the co-location satellite. First the orbit of the co-location satellite and the satellites of the GPS constellation were simulated by the SGP4 propagator for a period of one day with time step of one minute. Then the visibility is checked at every epoch. The availability of minimum four visible GPS satellites is necessary for coordinate determination by trilateration. For this a condition is developed in the Matlab code that checks minimum four visible GPS satellites at every epoch. If the condition is fulfilled at that epoch, the code proceeds and the coordinates of the co-location satellite are determined otherwise the program control jumps to next epoch and performs the same procedure test again until the condition is satisfied. For the data used for simulations, there are 31 satellites listed on the Celestrak website as operational satellites. According to [14], the total number of GPS satellites acquirable during a specific instant of time depends on the operational spare satellites available in orbit and also the number of satellite outages. 30 GPS satellites have been used for co-location satellite's coordinate determination.

### 5.1 Condition for visibility

As the satellites are continuously orbiting the Earth, there always is a possibility that the co-location satellite viewed by GPS satellites is blocked by the Earth. As we required four GPS satellites at every epoch, there might be a possibility that at one epoch only one or two GPS satellites can view the co-location satellite and at next epoch only three due to blockage by the Earth. To overcome this hurdle a visibility condition was developed that can be described by the figure below:

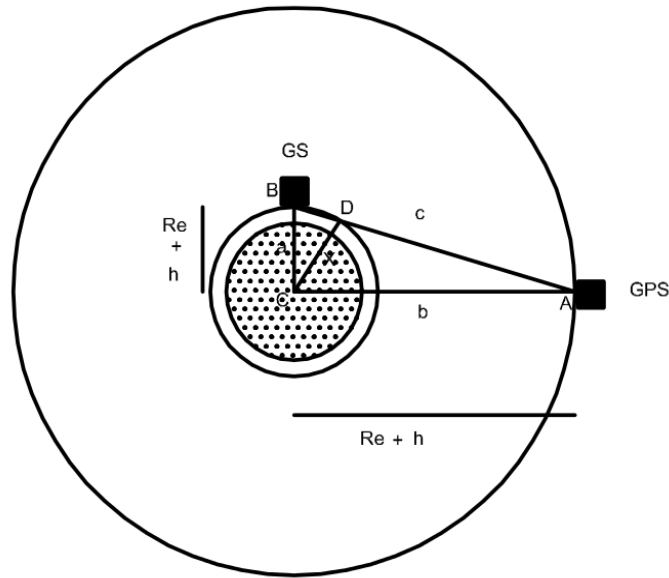


Figure 9: Visibility of a co-location satellite and a GNSS satellite

Figure 9 uses the Globalstar satellite as a co-location satellite and GPS satellite as a GNSS satellite. GS (Globalstar) and GPS satellites are orbiting the earth at the vector distance of  $a$  and  $b$  respectively, measured from the center of the Earth. The dotted inner circle is shown as the Earth, the smaller outer circle is the orbit of GS satellite while the bigger outer circle is the orbit of GPS satellite.  $a$  is the vector distance in km from the Earth's center to the GS satellite that is equivalent to the radius of Earth plus the altitude of satellite above the Earth's surface ( $Re+h$ ). The altitude of GS satellite is approximately 1400 km above the Earth's surface.  $b$  is the vector distance in km from the Earth's center to the GPS satellite. The GPS satellites are approximately at an altitude of 20200 km above the surface of the Earth.  $c$  is the vector distance in km from the GS satellite to the GPS satellite and is given by:

$$\vec{c} = |\vec{b} - \vec{a}| \quad (5-1)$$

The length of the perpendicular CD, denoted  $X$ , determines the visibility of the GS satellite by the GPS satellite.  $X$  should be greater than  $6378e3$ , the radius of the Earth, to allow visibility between GS and GPS. If  $X$  is less than the radius of the Earth this means the GS satellite is on the other side of the Earth or is below the horizon of GPS satellite.

Considering the units in km, the condition for visibility as a generalized solution for any geometry between GS and GPS satellite is

$$X \geq 6378 \quad (5-2)$$

as  $X$  is perpendicular to  $c$  so a right-angled triangle CBD is formed in Figure 9. The triangle CBD gives

$$\sin\beta = \frac{X}{|\vec{a}|} \quad (5-3)$$

$$X = |\vec{a}| \sin\beta \quad (5-4)$$

where  $\beta$  is the angle opposite to  $X$  in right-angled triangle CBD, expressed in degrees, and can be calculated by the dot product of vectors  $a$  and  $c$  as

$$\vec{a} \cdot \vec{c} = |\vec{a}| \cdot |\vec{c}| \cos\beta \quad (5-5)$$

$$\beta = \arccos\left(\frac{\vec{a} \cdot \vec{c}}{|\vec{a}| |\vec{c}|}\right) \quad (5-6)$$

After the condition for visibility is fulfilled, the least-squares estimation process starts for the position determination. How the least-squares is used for positions determination is described in next Chapter.

## 6 Least-Squares Estimation using GPS

The least-squares method is the most commonly used algorithm for position determination from pseudoranges, which is used to find the positions of four or more satellites. It is used to find the approximate solution of overdetermined systems. An overdetermined system is a set of equations having more equation than unknowns. The least-squared method determines an approximate overall solution that minimizes the sum of the squares of the errors made in the results of every equation within the system.

The simplified observation equations for the pseudoranges to four satellites in view of the receiver are given by [16] as:

$$P_1 = ((x_1 - x)^2 + (y_1 - y)^2 + (z_1 - z)^2)^{1/2} + c(t - t_1) \quad (6-1)$$

$$P_2 = ((x_2 - x)^2 + (y_2 - y)^2 + (z_2 - z)^2)^{1/2} + c(t - t_2) \quad (6-2)$$

$$P_3 = ((x_3 - x)^2 + (y_3 - y)^2 + (z_3 - z)^2)^{1/2} + c(t - t_3) \quad (6-3)$$

$$P_4 = ((x_4 - x)^2 + (y_4 - y)^2 + (z_4 - z)^2)^{1/2} + c(t - t_4) \quad (6-4)$$

the subscripts in the above equations denote the satellites. For 'n' equations, it can be written as

$$P_k = ((x_k - x)^2 + (y_k - y)^2 + (z_k - z)^2)^{1/2} + c(t - t_k) \quad (6-5)$$

where  $(x^k, y^k, z^k)$  is the position of satellites in view of the receiver,  $k=1,2,3,\dots$ ,  $k$  denotes the number of satellite,  $(x, y, z)$  are the unknown receiver coordinates and  $T, T^k$  are the receiver clock bias and the satellite 'k' clock bias respectively, added to the pseudorange to each visible satellite.

Ephemerids, part of navigation message broadcast by every GPS satellite, contains orbital information from which satellite position and timing information  $(x^k, y^k, z^k, \tau^k)$  can be computed. The unknown receiver position and time information  $(x, y, z, \tau)$  can be determined by the Least-Squares method. The Equation (6-5) contains the clock corrections for the satellite and the receiver which are expressed in meters by multiplying with the speed of light.

To make the calculations and computations simple, the timing information has been neglected in this project. So the Equation (6-5) becomes

$$P_k = ((x_k - x)^2 + (y_k - y)^2 + (z_k - z)^2)^{1/2} \quad (6-6)$$

The least-squares approach requires a linear system of equations and as the pseudorange Equation (6-6) is non-linear so this needs to be linearized.

Applying Taylor's expansion at a-priori position, the above observation equation gives the linearized equation:

$$P(x,y,z) = P(x_0, y_0, z_0) + (x - x_0) \frac{\partial P}{\partial x} + (y - y_0) \frac{\partial P}{\partial y} + (z - z_0) \frac{\partial P}{\partial z} \quad (6-7)$$

that includes only the first order terms. It can also be written as

$$P(x, y, z) = P(x_0, y_0, z_0) + \frac{\partial P}{\partial x} \Delta x + \frac{\partial P}{\partial y} \Delta y + \frac{\partial P}{\partial z} \Delta z \quad (6-8)$$

It is to be noted that the partial derivatives in above equation are calculated at provisional parameter value  $(x_0, y_0, z_0)$ , an initial estimate for the receiver position which is also known as a-priori value. The a-priori position of a receiver can be taken as  $(0, 0, 0)$ , the Earth's center, as an initial value. The corrections to these initial estimates, to obtain the receiver actual coordinates, can then be determined iteratively [15].

The partial derivative for the above equation can be determined as:

$$\frac{\partial P}{\partial x} = \frac{-(x - x_0)^2}{P_i} \quad (6-9)$$

$$\frac{\partial P}{\partial y} = \frac{-(y - y_0)^2}{P_i} \quad (6-10)$$

$$\frac{\partial P}{\partial z} = \frac{-(z - z_0)^2}{P_i} \quad (6-11)$$

in terms of the variables used in the MatLab code, the above partial derivatives can be written as:

$$\frac{\partial D_i}{\partial X_{GS}} = \frac{-(X_{GPS} - X_{GS})^2}{D_i} \quad (6-12)$$

$$\frac{\partial D_i}{\partial Y_{GS}} = \frac{-(Y_{GPS} - Y_{GS})^2}{D_i} \quad (6-13)$$

$$\frac{\partial D_i}{\partial Z_{GS}} = \frac{-(Z_{GPS} - Z_{GS})^2}{D_i} \quad (6-14)$$

where subscripts GPS and GS denotes the GPS and Globalstar satellites respectively. Substitution of these partial derivatives in Equation (6-8) gives

$$P(x, y, z) = P(x_0, y_0, z_0) + \frac{-(X_{GPS} - X_{GS})^2}{D_i} \Delta x + \frac{-(Y_{GPS} - Y_{GS})^2}{D_i} \Delta y + \frac{-(Z_{GPS} - Z_{GS})^2}{D_i} \Delta z \quad (6-15)$$

$$P(x, y, z) - P(x_0, y_0, z_0) = \frac{-(X_{GPS} - X_{GS})^2}{D_i} \Delta x + \frac{-(Y_{GPS} - Y_{GS})^2}{D_i} \Delta y + \frac{-(Z_{GPS} - Z_{GS})^2}{D_i} \Delta z \quad (6-16)$$

$P(x, y, z)$  is the observed pseudorange between the GPS satellite and the receiving satellite (in this case GS) calculated by the coordinates generated by the SGP4 propagator. It is also called an actual observation.  $P(x_0, y_0, z_0)$  is the observed pseudorange computed using provisional parameter values

for GS satellite. It is also called 'computed pseudorange' or 'calculated pseudorange' [16]. The measurement noise of 1mm was also added deliberately to the observed pseudorange.

Equation (6-16) can also be written as:

$$\Delta P = \frac{-(X_{GPS} - X_{GS})^2}{D_i} \Delta x + \frac{-(Y_{GPS} - Y_{GS})^2}{D_i} \Delta y + \frac{-(Z_{GPS} - Z_{GS})^2}{D_i} \Delta z \quad (6-17)$$

Now here  $\Delta P$  is called the Residual Observation and is defined as the difference between the actual observation and the observation computed using provisional parameter values[16].

In matrix form it can be written as:

$$\Delta P = \begin{bmatrix} \frac{-(X_{GPS} - X_{GS})}{D_i} & \frac{-(Y_{GPS} - Y_{GS})}{D_i} & \frac{-(Z_{GPS} - Z_{GS})}{D_i} \end{bmatrix} \begin{bmatrix} \Delta X \\ \Delta Y \\ \Delta Z \end{bmatrix} \quad (6-18)$$

Trilateration requires minimum three known points for three ranges. However, GPS point positioning requires 4 satellites for 4 pseudoranges[16] to eliminate the timing error introduced due to inaccurate receiver clocks. On the contrary, the pseudorange equations derived above does not contain the timing correction terms (to simplify the calculations and computations). In fact, these equations must be called range equations instead of pseudorange as there is no timing terms as they simply calculates the range between the known points. To generalize the solution where we have timing information and 4 satellites in view, the term pseudorange has been used in this description. So for a system of linear equation having  $m \geq 4$  satellites in view, equation (6-18) can be written as:

$$\begin{bmatrix} \Delta P_1 \\ \Delta P_2 \\ \Delta P_3 \\ \cdot \\ \cdot \\ \Delta P_m \end{bmatrix} = \begin{bmatrix} \frac{-(X_{GPS_1} - X_{GS})}{D_1} & \frac{-(Y_{GPS_1} - Y_{GS})}{D_1} & \frac{-(Z_{GPS_1} - Z_{GS})}{D_1} \\ \frac{-(X_{GPS_2} - X_{GS})}{D_2} & \frac{-(Y_{GPS_2} - Y_{GS})}{D_2} & \frac{-(Z_{GPS_2} - Z_{GS})}{D_2} \\ \frac{-(X_{GPS_3} - X_{GS})}{D_3} & \frac{-(Y_{GPS_3} - Y_{GS})}{D_3} & \frac{-(Z_{GPS_3} - Z_{GS})}{D_3} \\ \cdot & \cdot & \cdot \\ \cdot & \cdot & \cdot \\ \frac{-(X_{GPS_m} - X_{GS})}{D_m} & \frac{-(Y_{GPS_m} - Y_{GS})}{D_m} & \frac{-(Z_{GPS_m} - Z_{GS})}{D_m} \end{bmatrix} \begin{bmatrix} \Delta X \\ \Delta Y \\ \Delta Z \end{bmatrix} \quad (6-19)$$

Using matrix symbols it can be written as:

$$A x = l \quad (6-20)$$

Here 'A' is called the 'design matrix' that contains linear coefficients. These coefficients obtained by taking the partial derivative of every observation pseudorange with respect to each variable. The columns, 'n', of design matrix are of the same number as there are parameters and as much rows 'm' as there are satellites.

The 'x' is a column vector that contains the difference between the unknowns and a-priori values which gives the corrections to the a-priori values.

'l' is also a column vector that contains difference between the Observed and the computed pseudoranges.

A covariance matrix C is also needed here for the observations. Assuming uncorrelated pseudorange observations having same uncertainties, a unity matrix is used for simplicity [15]. Thus the covariance matrix for 'm=4' visible satellites look like this:

$$C = \begin{bmatrix} 1 & 0 & 0 & 0 \\ 0 & 1 & 0 & 0 \\ 0 & 0 & 1 & 0 \\ 0 & 0 & 0 & 1 \end{bmatrix} \quad (6-21)$$

To solve the least-squares system of equations, a MatLab function *lscov()* was used. The *lscov()* function takes design matrix 'A' and residual 'L' and returns the corrections to the a-priori value and the corresponding standard deviations 'dx'. As a first guess the a-priori value is taken as center of the Earth, (0, 0, 0), and design matrix is calculated at this point and passed to the *lscov()* function which returns the corrections 'x' and added to the a-priori value to be used for the next iteration. At next iteration the design matrix is again calculated with the new a-priori value and new corrections are generated. This process goes on until a threshold level of, let say, 1 cm is achieved. When the threshold level is achieved, the latitude and longitude are calculated from the estimated points at that epoch and then the programs jumps to next epoch to determine the next points with the same procedure.

### Converting estimated Cartesian coordinates to Geographic coordinates [15]

Considering the GRS80 system, the longitude of a point from a Cartesian coordinates is determined by

$$\lambda = \arctan\left(\frac{Y_{GS}}{X_{GS}}\right) \quad (6-22)$$

The calculation of latitude is not as easy as longitude and requires iterative solution. As GRS80 ellipsoid is used as an approximate shape of the earth, so we have semi-major axis,  $a = 6378.137$  km and semi-minor axis,  $b = 6356.7523141$  km.

So the latitude is calculated by :

$$\beta = \arctan\left(Z_{GPS} + \frac{a^2 - b^2}{b} \cdot \frac{\sin\beta_0}{V}\right) \quad (6-23)$$

where  $\beta_0$  is the longitude at previous iteration and is calculated by

$$\beta_0 = \arctan \frac{Z_{GPS}}{X_0} \quad (6-24)$$

where

$$X_0 = \sqrt{X^2 + Y^2} \quad (6-25)$$

and

$$V = \sqrt{1 + \frac{a^2 - b^2}{b^2} \cdot \cos^2 \beta} \quad (6-26)$$

When  $\beta$  is calculated, the difference between  $\beta$  and  $\beta_0$  is taken. If the difference is larger than a threshold level of  $1e-4$  than value of  $\beta$  is assigned to  $\beta_0$  and new iterations starts. This process is continues until specified threshold level is achieved and  $\beta$  is calculated.

When the latitude is determined the height of the object above the ellipsoid can be calculated by the following equations:

$$h = \frac{Z}{\sin \beta} - \frac{b}{V} \quad \text{if } (\beta) > 45^\circ \quad (6-27)$$

$$h = \frac{X_0}{\sin \beta} - \frac{a^2}{b} \quad \text{if } (\beta) < 45^\circ \quad (6-28)$$

## 7 Results and Discussions

The figures below show the comparisons of original and estimated position vectors for the Globalstar satellite. The original position vectors are the  $x$ ,  $y$ ,  $z$  values of position of the co-location satellite, in this case Globalstar, generated by propagating the TLE with the SGP4 for one day with time steps of one second. Thus we have 1440 positions of satellite. The estimated position vectors are  $x$ ,  $y$ ,  $z$  values of the positions determined by the GPS satellite network. During the estimation process a noise of 1 mm was added to the determined positions, This noise was generated by the `randn()` Matlab function that generates normally distributed pseudo- random numbers every time the code is simulated.

### Comparison of original and estimated positions vectors

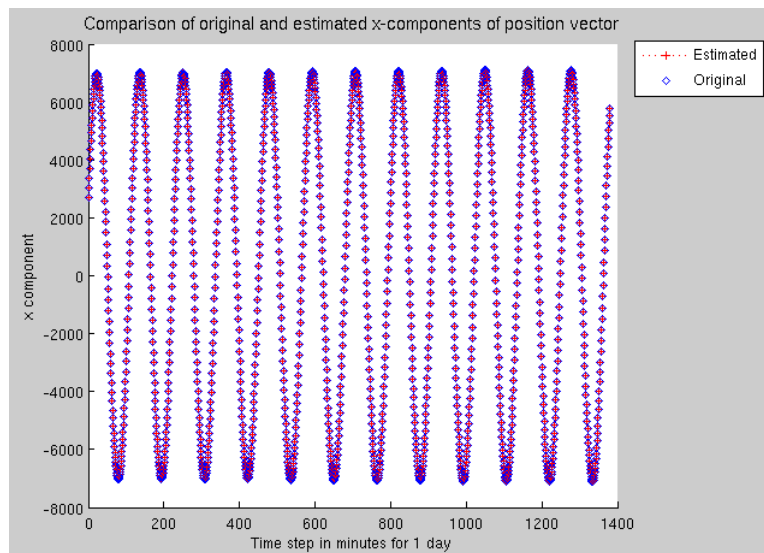


Figure 10: Comparison of original and estimated x-components of the position vector for Globalstar satellite

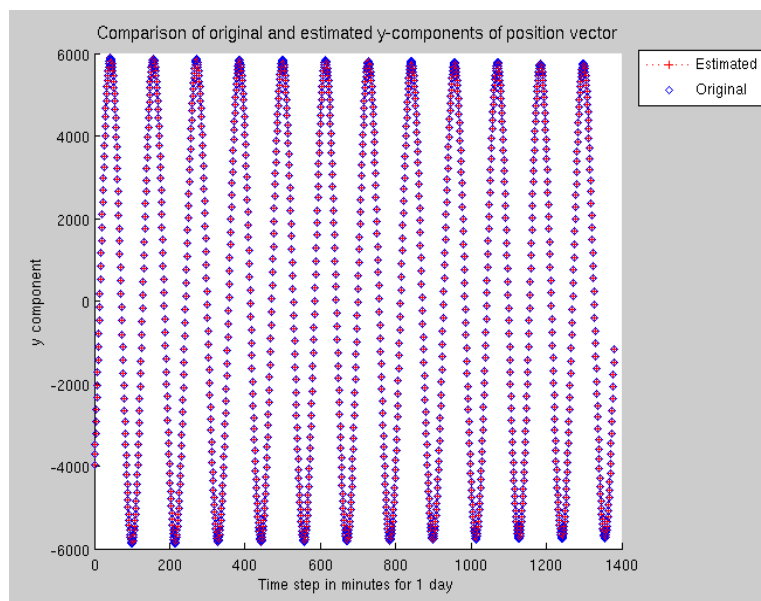


Figure 11: Comparison of original and estimated y-components of the position vector for Globalstar satellite

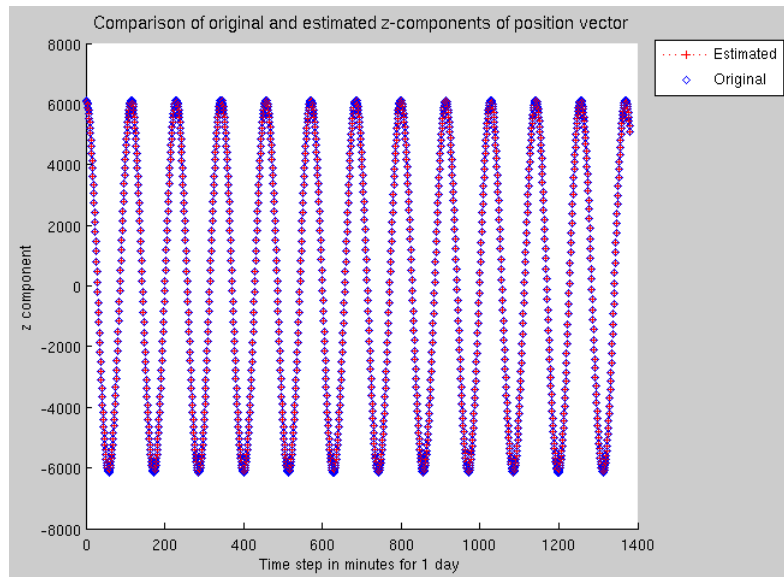


Figure 12: Comparison of original and estimated z-components of the position vector for Globalstar satellite

The results for other satellites were also similar so only the results for Globalstar satellite were shown. Figures 10, 11 and 12 shows that the original and estimated positions are very close to each other which gives the impression that the estimated positions are exactly the same. But actually there exists a difference due to the deliberately added measurement noise. This fact is obvious in the figures below that show the vector difference of original and estimated positions and also the standard deviations. These are shown for all the satellites.

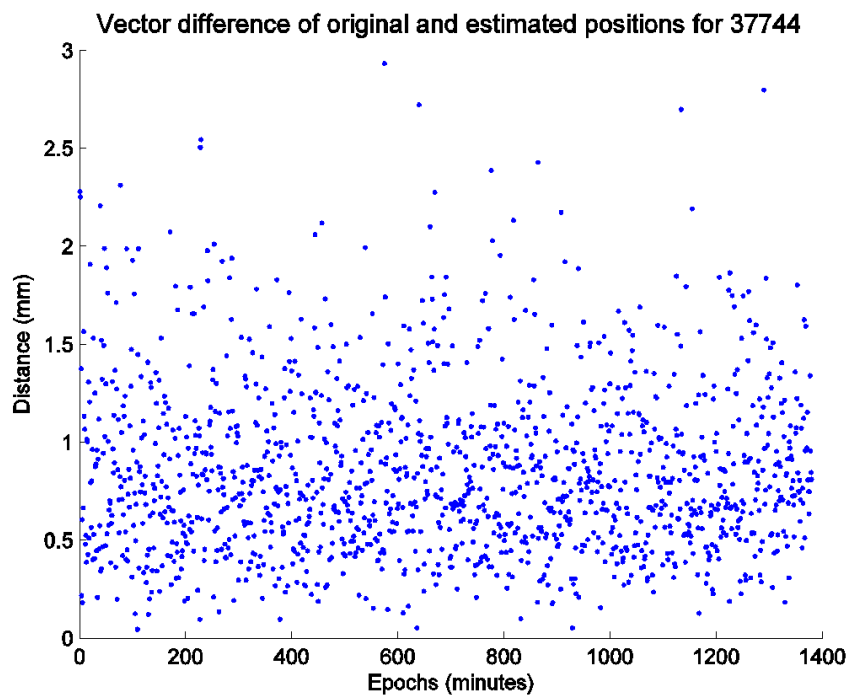


Figure 13: Vector difference of original and estimated coordinates for Globalstar

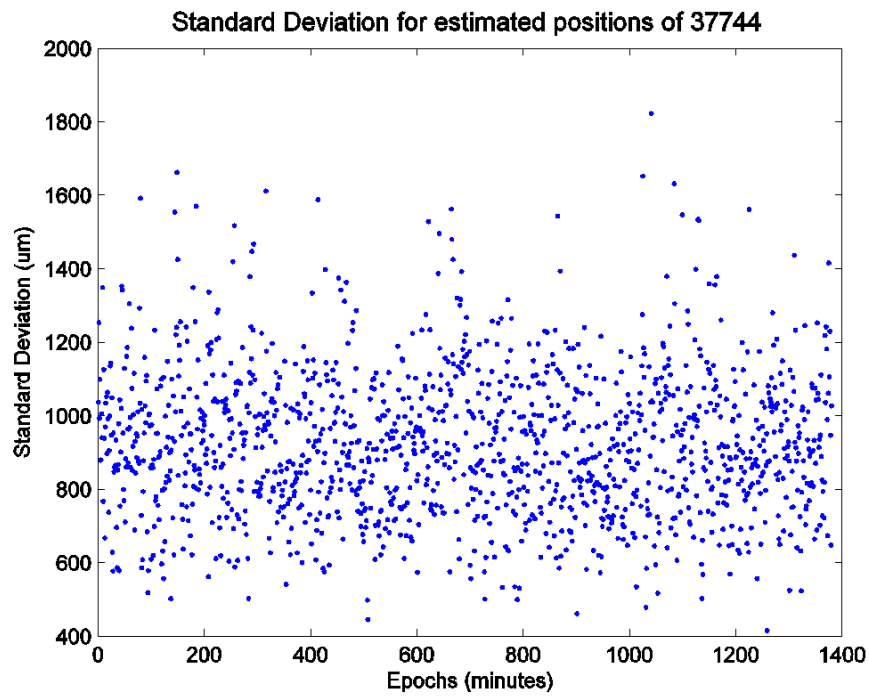


Figure 14: Standard deviations for estimated coordinates for Globalstar

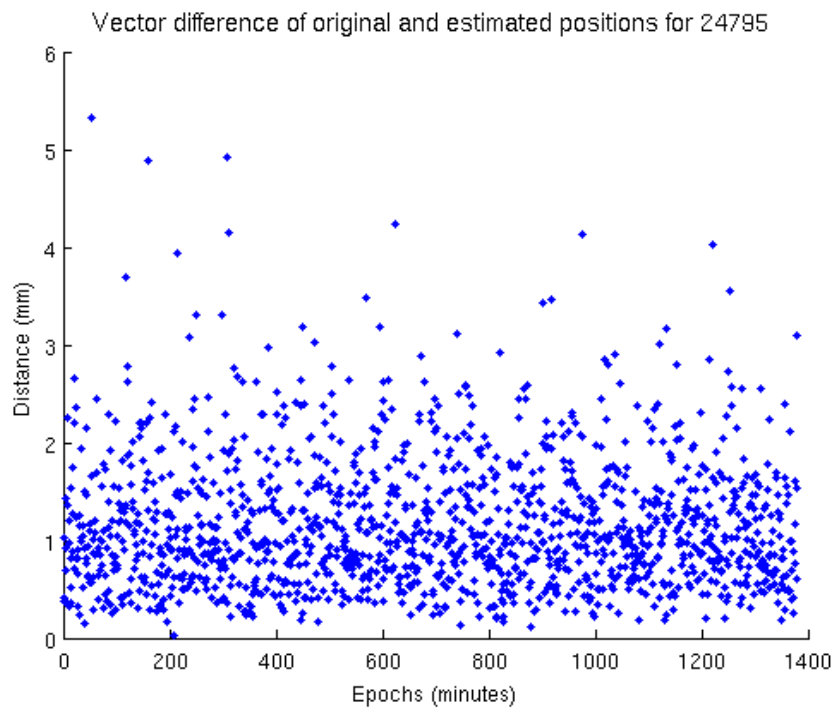


Figure 15: Vector difference of original and estimated coordinates for Iridium

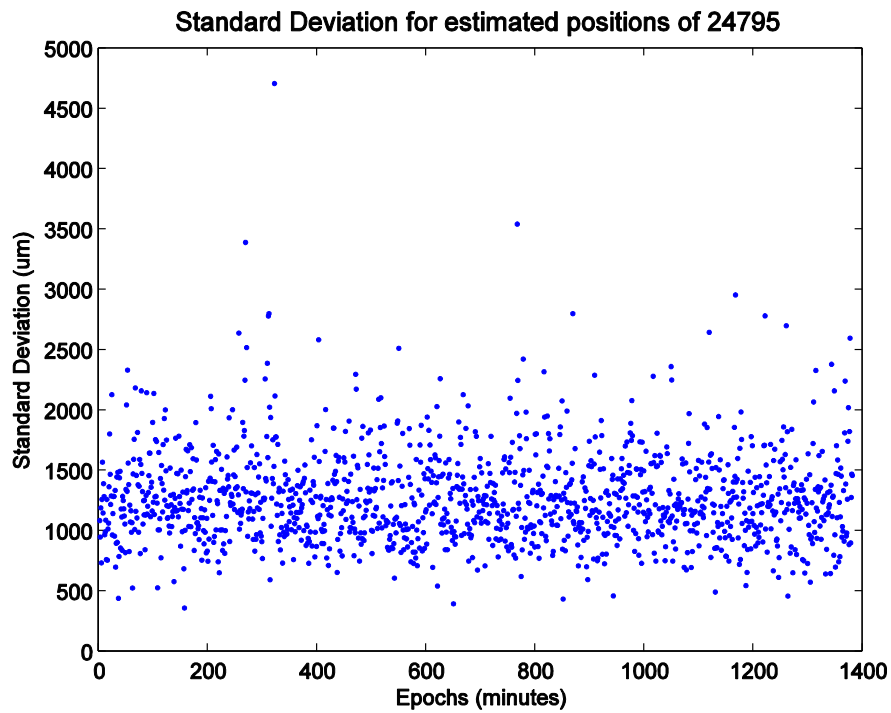


Figure 16: Standard deviations for estimated coordinates for Iridium

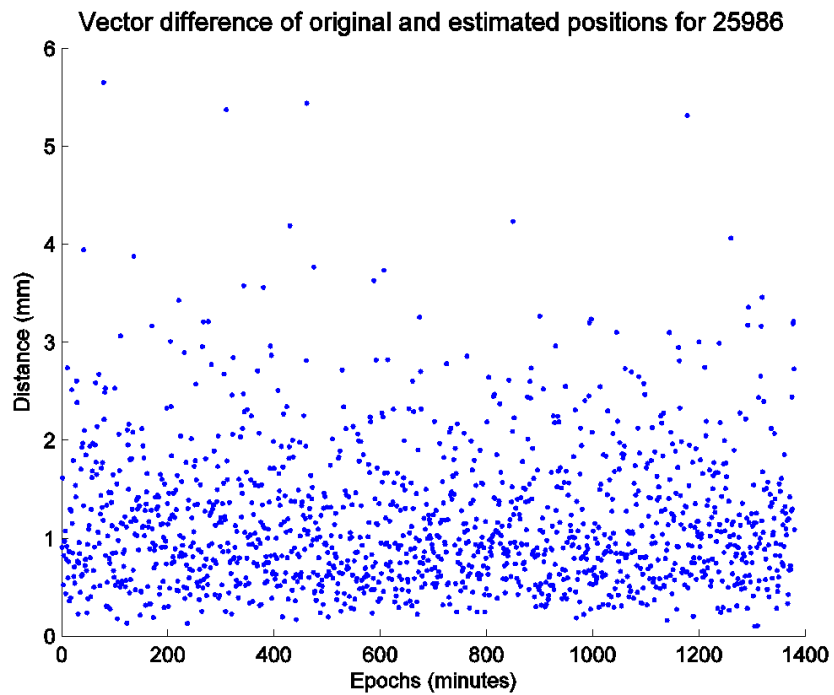


Figure 17: Vector difference of original and estimated coordinates for Orbcomm

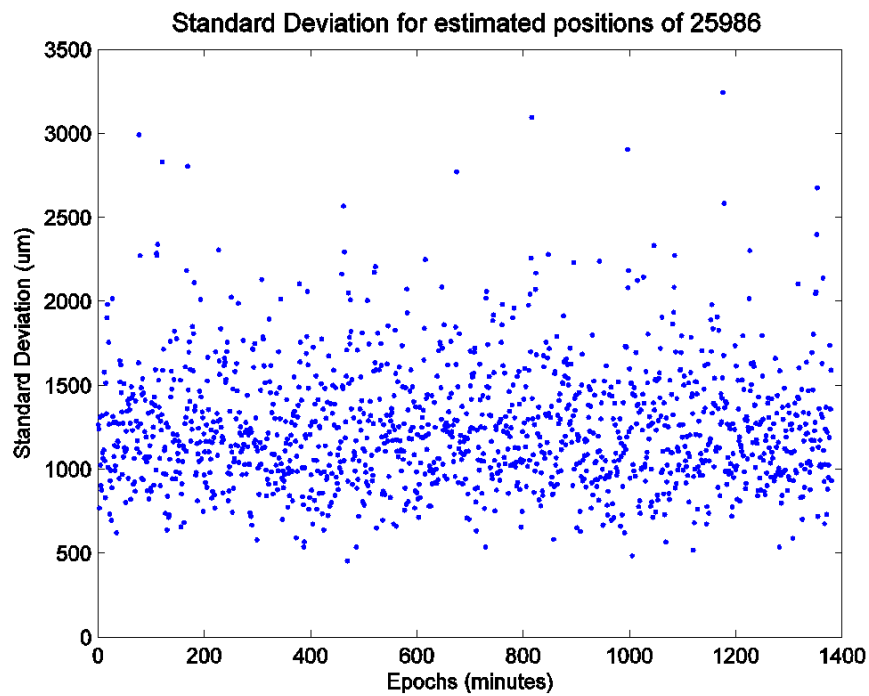


Figure 18: Standard deviations of estimated coordinates for Orbcomm

The Iridium and Orbcomm satellites both are at an altitude of almost 800 km that gives the higher values of  $\sigma$  and  $dd$ . The standard deviation is denoted by  $\sigma$  and the vector difference is denoted by  $dd$ .

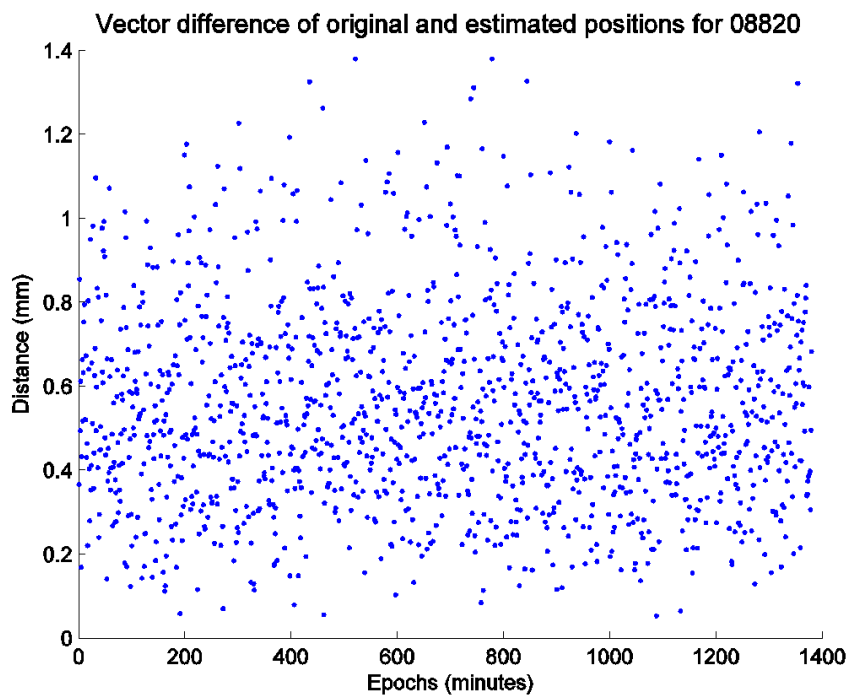


Figure 19: Vector difference of original and estimated coordinates for LAGEOS-1

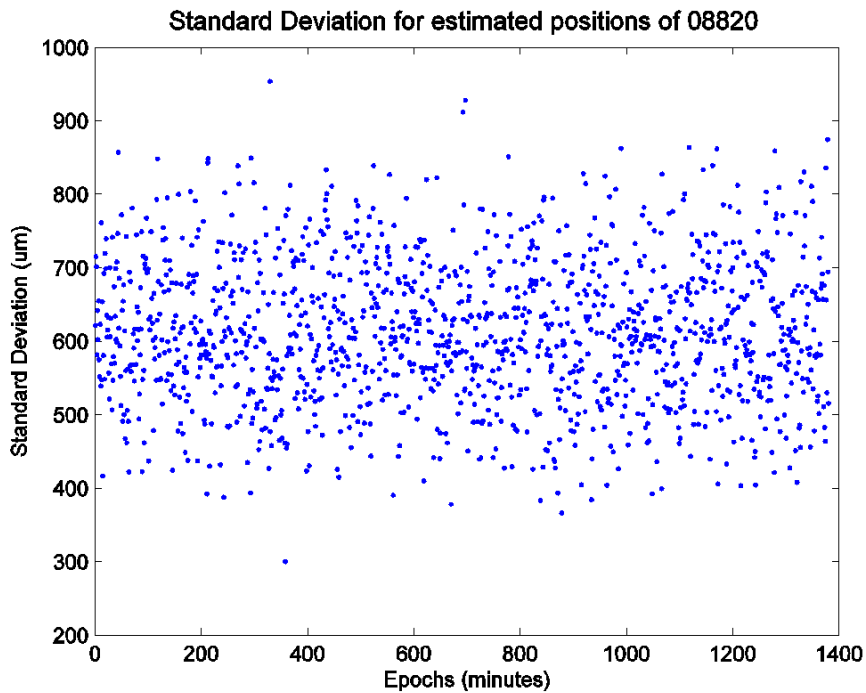


Figure 20: Standard deviations of estimated coordinates for LAGEOS-1

Table 5: Standard deviations of estimated positions

Satellite Name	NORAD Id	Max $\sigma$ (mm)	Mean $\sigma$ (mm)
Globalstar	37744	1.82	0.92
Iridium	24795	4.71	1.28
Orbcomm	29586	3.24	1.25
LAGEOS-1	08820	0.95	0.61

Table 6: Vector difference of original and estimated positions

Satellite Name	NORAD Id	Max dd(mm)	Mean dd(mm)
Globalstar	37744	2.93	0.85
Iridium	24795	5.32	1.17
Orbcomm	29586	5.65	1.16
LAGEOS-1	08820	1.38	0.56

Tables 5 and 6 present the standard deviations and vector difference, respectively for all the satellites. The maximum standard deviations and maximum vector difference are very low for LAGEOS-1 satellite. This is because the LAGEOS-1 satellite is at highest altitude of 6000 km, compared to other satellites, that contributes to better geometry with the GPS satellites and also provides visibility for more GPS satellites. The Globalstar satellite is at an altitude of 1400 km that

gives the second lowest deviations after the LAGEOS-1 satellite. Iridium and which are almost the same. This discussion leads to the conclusion that the higher orbital altitudes of co-location satellites will lead to the better results of estimation.

## **Part 2**

# **Coordinate determination of Co-location satellite by VLBI**

This section describes the coordinate determination of a co-location satellite by VLBI. The starting chapters present the theory required to build the foundations for the coordinate determination. Chapter 8 describes the light-time equation, Chapter 9 presents theory about Geometric Dilution of Precision (GDOP) and Chapter 10 discuss about the VLBI technique in general. Chapter 10 presents the whole process of estimating the positions of co-location satellite based on the theory of previous chapters. It also includes the programme flow of the MatLab code that used to predict the positions. Actually, the whole discussion in this chapter goes according to the code flow control and the subsequent equations needed in the code are also derived step by step according to the code flow. For example, the equations for the calculation of a a-priori value for the co-location satellite are derived at the point where programme flow needed it. Also any decision making is also stated accordingly.

## 8 Light-Time Equation

The light-time equation calculates the signal elapsed time from the satellite to the ground station or vice versa. It also takes into account the correction due to relativistic effects. The light-time equation for Quasars also includes the curved wave front effects along with the relativistic effects. The satellite light-time equation is acquired from Equation (8-67) in [21] which is expressed in local geocentric frame of reference. Local geocentric frame of reference is the more convenient way for locating near-Earth orbiting satellites. Satellites in deep-space missions are more conveniently located in solar-system barycentric frame of reference. The light-time solution expressed in solar-system barycentric space-time frame of reference for deep-space satellite is also given in [21]. As our co-location satellite is a near-Earth satellite, the light-time solution expressed in local geocentric frame of reference is given as:

$$t_3 - t_2 = \frac{r_{23}}{c} + \frac{(1+\gamma)\mu_E}{c^3} \ln \left[ \frac{r_2 + r_3 + r_{23}}{r_2 + r_3 - r_{23}} \right] \quad (8-1)$$

Here  $t_3$  is the signal reception time at a tracking ground station, like VLBI station, or a receiving satellite.

$t_2$  is the transmit time at the satellite.

$\mu_E$  is the gravitational constant of the Earth given by  $3.9860044 \times 10^{14}$ .

$\gamma$  is the relativistic constant. For the case of general relativity it is 1.

$r_2$  is the distance between the geocenter and the satellite.

$r_3$  is the distance between the geocenter and the ground tracking station.

$r_{23}$  is the distance between the ground tracking station and the satellite.

This is a down-leg light path that starts with the actual position of satellite at transmit time  $t_2$  and ends at the ground tracking station' or other receiving satellite at received time  $t_3$ . For the case of up-leg light path the up-leg light-time equation can be found by replacing 3 with 2 and 2 with 1 [21]. This light-time equation is formulated in the non-inertial frame of reference and is in a local geocentric frame of reference and also is non-rotating with respect to the Solar-System barycentric space-time frame of reference [21].

## 9 Geometric Dilution of Precision (GDOP)

The Geometric Dilution of Precision (GDOP) is a numerical measurement used in GNSS that takes into account the geometry of satellites for the purpose of precise positioning. Geometry of visible satellites to the receiver tells about how the satellites are separated with each other on the sky, which plays an important role in positioning. There are two types of errors that can affect the GPS positioning: the errors due the range measurement and errors due to the satellites geometry. Although the errors due to range measurements can be mitigated by the use of WAAS (Wide Area Augmentation System), post-processing and averaging, but satellite geometry still contributes to the errors [20].

When the visible GNSS satellites are far apart from each other having wider angles, the geometry is said to be strong and the DOP values are lower. On the contrary, the closer angle of separation contributes to weak geometry and higher DOP values that leads to the errors in the positioning. The figure below illustrates the concept of GDOP having satellite geometries for good and bad GDOPs [18].

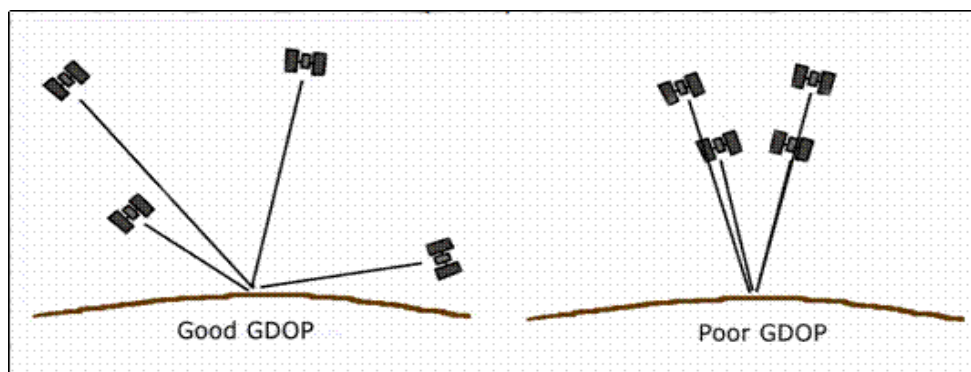


Figure 21: GPS satellites geometries for good and bad GDOPs [22]

Although the GDOP concept is related to the GNSS, but it can also be applied to other systems that rely on various sites located apart geographically. This concept of GDOP is utilized here on the VLBI sites that take part in position determination of co-location satellite where the good geometry of visible VLBI sites is necessary for precise orbit determination.

There are different DOP levels within the range 0-20 that provides different levels of accuracy for variety of applications. All these DOP levels with their description are summarized in the Table 6.

Table 7: Different DOP values with their ratings and description [18]

<b>DOP value</b>	<b>Rating</b>	<b>Description</b>
<1	Ideal	This is the highest possible confidence level to be used for applications demanding the highest possible precision at all times.
1-2	Excellent	At this confidence level, positional measurements are considered accurate enough to meet all but the most sensitive applications.
2-5	Good	Represents a level that marks the minimum appropriate for making business decisions. Positional measurements could be used to make reliable in-route navigation suggestions to the user.
5-10	Moderate	Positional measurements could be used for calculations, but the fix quality could still be improved. A more open view of the sky is recommended.
10-20	Fair	Represents a low confidence level. Positional measurements should be discarded or used only to indicate a very rough estimate of the current location.
>20	Poor	At this level, measurements are inaccurate by as much as 300 meters with a 6 meter accurate device ( $50 \text{ DOP} \times 6 \text{ meters}$ ) and should be discarded.

The GDOP is calculated by the formula given below:

$$GDOP = \sqrt{\text{tr}\{(A^T A)^{-1}\}} \quad (9-1)$$

Where 'tr' in the above equation shows the trace of matrix and 'A' denotes the design matrix that contains linear coefficients as in Equation (6-19).

## 10 VLBI for spacecraft tracking

VLBI (Very Long Base Line Interferometry) is an interferometric technique developed for radio astronomy with the purpose to improve the angular resolution. It is an astronomical interferometer that consists of two or more telescopes, relatively at very large distances of several thousands of kilometers, combined together to present a telescope of the same diameter as the distance between them, thus improving the angular resolution of the system. The VLBI technique was primarily developed for the observation of extragalactic radio sources such as Quasars but nowadays it is also been widely used for the observation and tracking of near-Earth and deep-space spacecraft.

### 10.1 Principle of VLBI observation

The primary observable of the VLBI is the measure of the difference in time of the received signals of a plane wavefront from a distant radio source at the two stations on the Earth [23]. This can be described by the figure below.

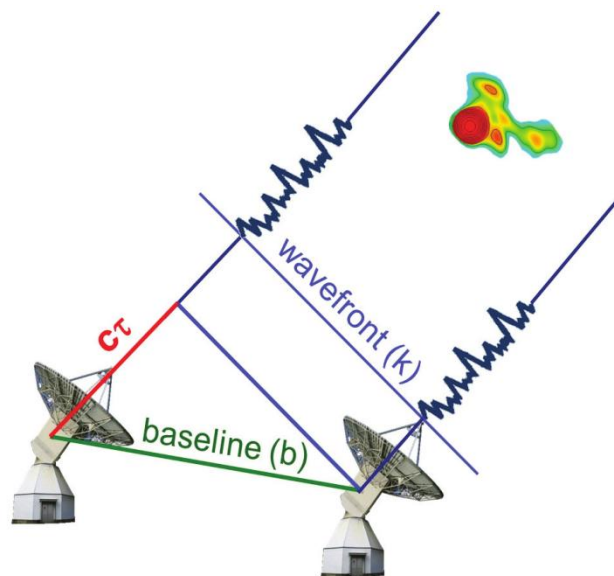


Figure 22: The VLBI observation of extragalactic radio source [23].

Figure 22 shows that the plane wavefront being received by the two radio telescopes operating in the VLBI mode. The extragalactic sources are at a great distance, several billion light-years, which is assumed as infinite and the wavefront of the emitted signal by these sources is approximated as a plane wave when received at the antennas of the two telescopes. The baseline 'b' is the distance between the two telescopes that incorporates a delay of signal reception at one of the telescope. This time delay is given in the form of geometric distance as ' $c\tau$ '.

If the object to be tracked is the near-earth satellite than the wavefront of the signal transmitted from the satellite is considered as a curved wave due to relatively a small distance. The signal delay

due to a curved wave front arriving at the two antennas should also be taken into account along with the satellite motion which relatively moves faster than quasars due to the small distance between the Earth and the satellite.

### 10.2 VLBI delay model

The VLBI delay model (observation equation) is a mathematical model that takes into account the delays in signal due to geometry, earth rotation and atmosphere (ionosphere, troposphere). For extragalactic sources a very famous delay model known as a 'consensus model' is based on the plane wave approximation is recommended by the IERS and is given by [23]:

$$-c\tau = b \cdot k + \Delta\tau_{clock} + \Delta\tau_{trop} + \Delta\tau_{iono} + \Delta\tau_{relativistic} \quad (10-1)$$

where,

$c$  = the velocity of light in vacuum,

$k$  = the unit source vector which defined in a space-fixed, barycentric and equatorial celestial system,

$b$  = the baseline vector of the VLBI stations which is defined in an

Earth-fixed, geocentric, equatorial terrestrial coordinate system,

$\Delta\tau_{clock}$  = the delay correction due to the synchronization and frequency discrepancies of atomic clocks relative to a fixed clock,

$\Delta\tau_{trop}$  = the troposphere delay correction,

$\Delta\tau_{iono}$  = the ionosphere delay correction and

$\Delta\tau_{relativistic}$  = the delay corrections due to the relativistic effects.

As our tracking object is a near-Earth spacecraft which is considered as a finite distance, a finite VLBI delay model was formulated. For the sake of simplicity, only a signal time delay due to different arrival times is considered in VLBI delay model for this task while Earth rotation, relativistic and atmospheric delays were discarded. The model is formulated in local geocentric non-inertial frame of reference, ECEF (Earth Centered Earth Fixed).

# 11 Coordinates determination by VLBI

The coordinates of a co-location satellite can also be determined by the VLBI network of ground stations. The stations are chosen such that they are spread all over the world to provide maximum visibility for accurate coordinate determination.

The selected VLBI station's names and their geographical coordinates are given in the Table 8:

Table 8: VLBI stations location information

Sr. no.	Station ID	Country	Continent	Lat. , long. (degrees)
1	Urumqi	China	Asia	43.4712N, 87.1779E
2	Tsukuba	Japan	Asia	36.1031N, 140.0887E
3	Hartrao	South Africa	Africa	25.8889S, 27.6854E
4	Parkes	Australia	Australia	32.9979S, 148.2646E
5	Westford	USA	North America	42.6129N, 71.4938 W
6	Greenbelt	USA	North America	39.0219N, 76.8265W
7	Onsala	Sweden	Europe	57.3958N, 11.9263E
8	Ny-Ålesund	Norway	Europe	78.5546N, 11.5155E
9	Tigoconc	Chile	South America	36.5037S, 73.0131W
10	O' Higgins	Antarctica	Antarctica	63.3209S, 57.9008W
11	Fortaleza	Brazil	South America	3.8777S, 38.4259W
12	Kokee Park	USA	North America	22.1260N, 159.6650S
13	Noto	Italy	Europe	36.8761N, 14.9890E
14	Badary	Russia	Asia	51.7667N, 120.2333E
15	Zelenchk	Russia	Asia	43.7833N, 41.5667E
16	Yaragadee	Australia	Australia	29.0247S, 115.2049E
17	Brewster	USA	North America	48.1312N, 119.6833W
18	Yebes	Spain	Europe	40.5241N, 3.0894W
19	Svetloe	Russia	Asia	60.5323N, 29.7819E
20	Sainte Croix	USA	North America	17.7566N, 64.5836W
21	Kitt Peak	USA	North America	31.9563N, 111.6124W

All these VLBI stations are shown in Figure 23 according to their serial number in the table above.

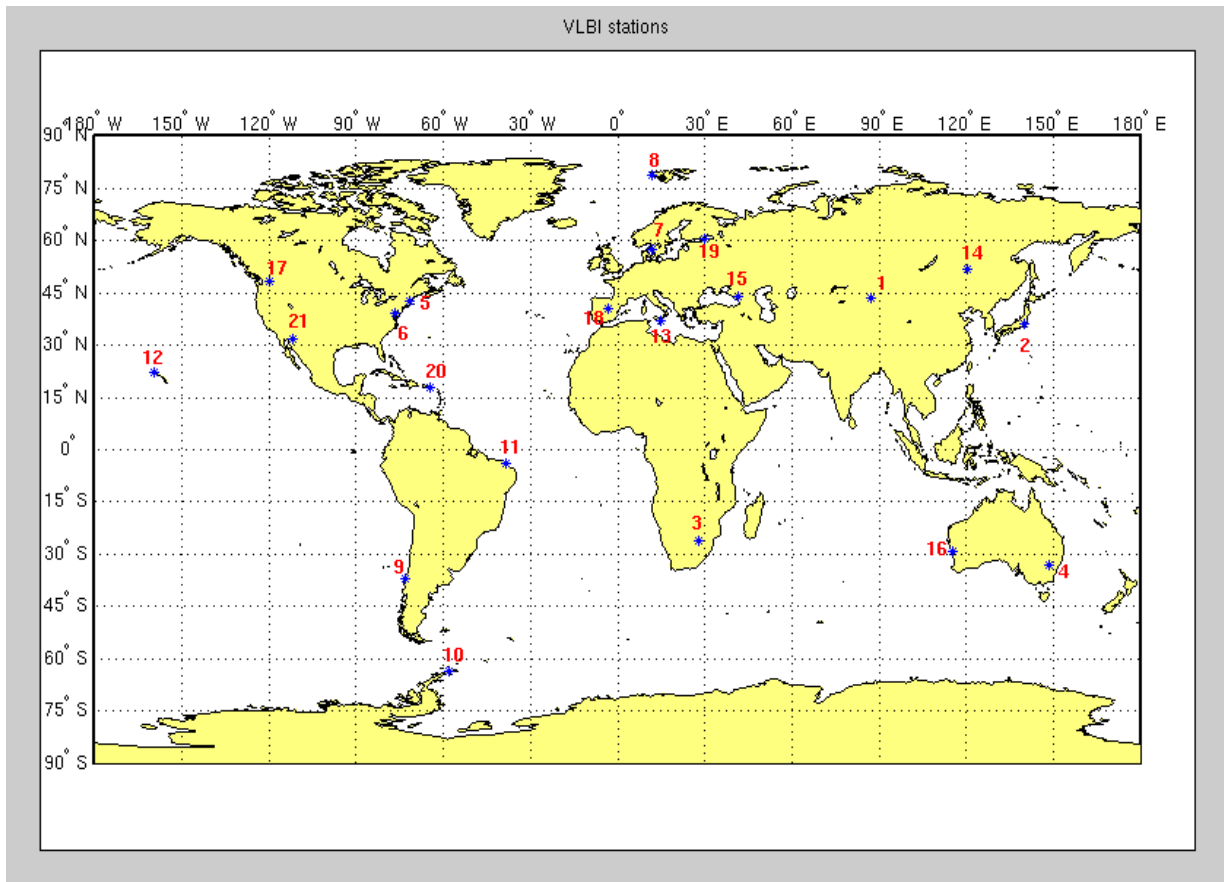


Figure 23: VLBI stations location plotted on the map

Like in the GNSS case we also need at least four observation equations for co-location satellite coordinate determination by VLBI stations. The VLBI technique requires two radio telescopes for a single observation. A network of three radio telescopes forms three combinations of two stations giving three base-lines hence three observation equations which are still not fulfilling the requirements of four observation equations. Therefore a network of four or more radio telescopes is necessary to get at least four observation equations. Network of four radio telescopes gives six combinations of two stations and hence six baselines which fulfills the requirements.

### 11.1 VLBI delay in terms of Light-time equation

The satellite down-leg light-time equation in local geocentric space-time frame of reference is discussed in Chapter 8 and is given by Equation (8-1):

$$t_3 - t_2 = \frac{r_{23}}{c} + \frac{(1+\gamma)u_E}{c^3} \ln \left[ \frac{r_2 + r_3 + r_{23}}{r_2 + r_3 - r_{23}} \right] \quad (11-1)$$

The VLBI time delay is given by

$$\Delta\tau_{AB} = t_B - t_A \quad (11-2)$$

where,  $t_B = t_3 - t_2$ , is the light-time solution at station B and  
 $t_A = t_3 - t_2$ , is the light-time solution at station A.

so the Equation (11-2) becomes

$$\Delta\tau_{AB} = (t_3 - t_2)_B - (t_3 - t_2)_A \quad (11-3)$$

here the subscripts A and B denote the stations A and B respectively.

substituting light-time equation in Equation (11-3), we get

$$\Delta\tau_{AB} = \left( \frac{r_{23}}{c} + \frac{(1+\gamma)u_E}{c^3} \ln \left[ \frac{r_2 + r_3 + r_{23}}{r_2 + r_3 - r_{23}} \right] \right)_B - \left( \frac{r_{23}}{c} + \frac{(1+\gamma)u_E}{c^3} \ln \left[ \frac{r_2 + r_3 + r_{23}}{r_2 + r_3 - r_{23}} \right] \right)_A \quad (11-4)$$

In the above equation the subscript 2 refers to the co-location satellite and 3 refers to station A if the light time solution is to be determined for station A, or refers to station B if the light time solution is to be determined for station B. So Equation (11-4) transforms to:

$$\Delta\tau_{AB} = \left( \frac{r_{SB}}{c} + \frac{(1+\gamma)u_E}{c^3} \ln \left[ \frac{r_S + r_B + r_{SB}}{r_S + r_B - r_{SB}} \right] \right) - \left( \frac{r_{SA}}{c} + \frac{(1+\gamma)u_E}{c^3} \ln \left[ \frac{r_S + r_A + r_{SA}}{r_S + r_A - r_{SA}} \right] \right) \quad (11-5)$$

This is more understandable with reference to stations A and B.

## 11.2 Least-Squares Estimation for VLBI

In Chapter 6, the coordinates of co-location satellite were determined by the least-square approach from the observation equations of pseudoranges between the co-location satellite and GNSS satellites. The nonlinear observation pseudorange equations were linearized by applying the Taylor's theorem which is a primary requirement for the least-squares method. The coefficient of design matrix for the least-squares were obtained by partial differentiation of linearized observation equation by the unknown coordinate variables of co-location satellite, initially at a-priori value.

The coordinates of co-location satellite by VLBI approach can be determined in the slightly different way, where the observation equations are the VLBI delay rather than the pseudorange equations for the GPS case. The coefficients of the design matrix, for the least-squares, are obtained by partial differentiation of the VLBI delay observation equations by the co-location satellite unknown coordinate variables (XS,YS,ZS).

The partial differentiation of Equation (11-5) with respect to XS, YS and ZS respectively, is given by:

$$\frac{\partial \Delta\tau_{AB}}{\partial X_S} = \frac{\partial}{\partial X_S} \left( \left( \frac{r_{SB}}{c} + \frac{(1+\gamma)u_E}{c^3} \ln \left[ \frac{r_S + r_B + r_{SB}}{r_S + r_B - r_{SB}} \right] \right) - \left( \frac{r_{SA}}{c} + \frac{(1+\gamma)u_E}{c^3} \ln \left[ \frac{r_S + r_A + r_{SA}}{r_S + r_A - r_{SA}} \right] \right) \right) \quad (11-6)$$

⇒

$$\begin{aligned} \frac{\partial \Delta\tau_{AB}}{\partial X_S} &= \frac{1}{c} \frac{(X_S - X_B)}{r_{SB}} + \frac{(1+\gamma)\mu_E}{c^3} \left( \frac{-2}{(r_S^2 + r_B^2 - r_{SB}^2 + 2r_B r_S)} \left( \left( X_S \left( \frac{r_{SB}}{r_S} \right) + (X_B - X_S) \left( \frac{r_S}{r_{SB}} \right) \right) + (X_B - X_S) \left( \frac{r_B}{r_{SB}} \right) \right) \right) \\ &- \frac{1}{c} \frac{(X_S - X_A)}{r_{SA}} - \left( \frac{(1+\gamma)\mu_E}{c^3} \left( \frac{-2}{(r_S^2 + r_A^2 - r_{SA}^2 + 2r_A r_S)} \left( \left( X_S \left( \frac{r_{SA}}{r_S} \right) + (X_A - X_S) \left( \frac{r_S}{r_{SA}} \right) \right) + (X_A - X_S) \left( \frac{r_A}{r_{SA}} \right) \right) \right) \right) \end{aligned} \quad (11-7)$$

similarly with respect to Ys

$$\frac{\partial \Delta\tau_{AB}}{\partial Y_S} = \frac{\partial}{\partial Y_S} \left( \left( \frac{r_{SB}}{c} + \frac{(1+\gamma)\mu_E}{c^3} \ln \left[ \frac{r_S + r_B + r_{SB}}{r_S + r_B - r_{SB}} \right] \right) - \left( \frac{r_{SA}}{c} + \frac{(1+\gamma)\mu_E}{c^3} \ln \left[ \frac{r_S + r_A + r_{SA}}{r_S + r_A - r_{SA}} \right] \right) \right) \quad (11-8)$$

⇒

$$\begin{aligned} \frac{\partial \Delta\tau_{AB}}{\partial Y_S} &= \frac{1}{c} \frac{(Y_S - Y_B)}{r_{SB}} + \frac{(1+\gamma)\mu_E}{c^3} \left( \frac{-2}{(r_S^2 + r_B^2 - r_{SB}^2 + 2r_B r_S)} \left( \left( Y_S \left( \frac{r_{SB}}{r_S} \right) + (Y_B - Y_S) \left( \frac{r_S}{r_{SB}} \right) \right) + (Y_B - Y_S) \left( \frac{r_B}{r_{SB}} \right) \right) \right) \\ &- \frac{1}{c} \frac{(Y_S - Y_A)}{r_{SA}} - \left( \frac{(1+\gamma)\mu_E}{c^3} \left( \frac{-2}{(r_S^2 + r_A^2 - r_{SA}^2 + 2r_A r_S)} \left( \left( Y_S \left( \frac{r_{SA}}{r_S} \right) + (Y_A - Y_S) \left( \frac{r_S}{r_{SA}} \right) \right) + (Y_A - Y_S) \left( \frac{r_A}{r_{SA}} \right) \right) \right) \right) \end{aligned} \quad (11-9)$$

similarly also with respect to Zs

$$\frac{\partial \tau_{AB}}{\partial Z_S} = \frac{\partial}{\partial Z_S} \left( \left( \frac{r_{SB}}{c} + \frac{(1+\gamma)\mu_E}{c^3} \ln \left[ \frac{r_S + r_B + r_{SB}}{r_S + r_B - r_{SB}} \right] \right) - \left( \frac{r_{SA}}{c} + \frac{(1+\gamma)\mu_E}{c^3} \ln \left[ \frac{r_S + r_A + r_{SA}}{r_S + r_A - r_{SA}} \right] \right) \right) \quad (11-10)$$

⇒

$$\begin{aligned} \frac{\partial \tau_{AB}}{\partial Z_S} &= \frac{1}{c} \frac{(Z_S - Z_B)}{r_{SB}} + \frac{(1+\gamma)\mu_E}{c^3} \left( \frac{-2}{(r_S^2 + r_B^2 - r_{SB}^2 + 2r_B r_S)} \left( \left( Z_S \left( \frac{r_{SB}}{r_S} \right) + (Z_B - Z_S) \left( \frac{r_S}{r_{SB}} \right) \right) + (Z_B - Z_S) \left( \frac{r_B}{r_{SB}} \right) \right) \right) \\ &- \frac{1}{c} \frac{(Z_S - Z_A)}{r_{SA}} - \left( \frac{(1+\gamma)\mu_E}{c^3} \left( \frac{-2}{(r_S^2 + r_A^2 - r_{SA}^2 + 2r_A r_S)} \left( \left( Z_S \left( \frac{r_{SA}}{r_S} \right) + (Z_A - Z_S) \left( \frac{r_S}{r_{SA}} \right) \right) + (Z_A - Z_S) \left( \frac{r_A}{r_{SA}} \right) \right) \right) \right) \end{aligned} \quad (11-11)$$

The above partial derivatives are the coefficient of the design matrix for one row, obtained for one baseline between stations A and B. The partial derivatives for other baselines, between stations B and C, C and D and so on, can be obtained by simply changing the subscripts A and B in above equations by the corresponding stations of other baselines.

### 11.3 Determination of the a-priori satellite position

The determination of the a-priori value for satellite in the least-square approach is a first step towards satellite coordinate determination with VLBI tracking. In Chapter 6 the a-priori value was selected as (0, 0, 0), center of the Earth, for satellite coordinate determination with GPS. The a-priori value was updated at each iteration step until the solution converged to a predefined threshold value of 1 cm. Selecting (0, 0, 0,) as a-priori value in VLBI case resulted in non-converged solutions. Some of the solutions that converged showed unrealistic numbers that fell in far apart form the actual satellite position. So there was a need of developing a new method of finding a reasonable a-priori value that could converge to a predefined threshold in reasonable iterations.

The a-priori position in the direction of satellite some 20000 km above the surface of the Earth would be a best guess. So we need direction vectors from the two VLBI stations, which can see the satellite simultaneously at the same epoch, in the direction of satellite and coincides beyond the satellite. A minimum elevation mask of 5° is selected for satellite visibility by the two VLBI stations.

Suppose the two VLBI stations 1 and 2 that can see the satellite have elevations  $\varepsilon_1$  and  $\varepsilon_2$  respectively and azimuth  $\alpha_1$  and  $\alpha_2$  respectively. In the topocentric coordinate system the direction vectors towards satellite are:

$$r_{i-1s}^{T_1} = \begin{bmatrix} \cos\varepsilon_1 \sin\alpha_1 \\ \cos\varepsilon_1 \cos\alpha_1 \\ \sin\varepsilon_1 \end{bmatrix}_{3 \times 1} \quad (11-12)$$

$$r_{i-2s}^{T_2} = \begin{bmatrix} \cos\varepsilon_2 \sin\alpha_2 \\ \cos\varepsilon_2 \cos\alpha_2 \\ \sin\varepsilon_2 \end{bmatrix}_{3 \times 1} \quad (11-13)$$

These direction vectors are given in matrix form with dimensions 3x1. Here 'r' denotes the direction vectors. The superscripts T1 and T2 denote the topocentric coordinate system for stations 1 and 2 respectively. That means the direction vectors are defined for stations 1 and 2 separately according to their respective topocentric coordinates. The subscripts 'i' denotes the topocentric coordinates (u, v, w), 1s for station 1. Also topocentric coordinates (u, v, w), 2s for station 2.

Now we need to rotate from the topocentric coordinate system to the geocentric Earth-fixed system, ECEF. This is achieved by the following rotation matrix.

$$R_{ij-T_1}^E = \begin{bmatrix} -\sin\lambda_1 & -\sin\phi_1 \cos\lambda_1 & \cos\phi_1 \cos\lambda_1 \\ \cos\lambda_1 & -\sin\phi_1 \sin\lambda_1 & \cos\phi_1 \sin\lambda_1 \\ 0 & \cos\phi_1 & \sin\phi_1 \end{bmatrix}_{3 \times 3} \quad (11-14)$$

$$R_{ijT_2}^E = \begin{bmatrix} -\sin\lambda_2 & -\sin\phi_2 \cos\lambda_2 & \cos\phi_2 \cos\lambda_2 \\ \cos\lambda_2 & -\sin\phi_2 \sin\lambda_2 & \cos\phi_2 \sin\lambda_2 \\ 0 & \cos\phi_2 & \sin\phi_2 \end{bmatrix}_{3 \times 3} \quad (11-15)$$

so the rotated direction vectors in the ECEF coordinate system are given by:

$$r_{i1s}^E = R_{ijT_1}^E \cdot r_{j1s}^{T_1} \quad (11-16)$$

$$r_{i2s}^E = R_{ijT_2}^E \cdot r_{j2s}^{T_2} \quad (11-17)$$

substituting values in (11-16) and (11-17) gives the following direction vectors in Earth fixed coordinates.

$$r_{i1s}^E = \begin{bmatrix} -\sin\lambda_1 \cos\varepsilon_1 \sin\alpha_1 - \sin\phi_1 \cos\lambda_1 \cos\varepsilon_1 \cos\alpha_1 + \cos\phi_1 \cos\lambda_1 \sin\varepsilon_1 \\ \cos\lambda_1 \cos\varepsilon_1 \sin\alpha_1 - \sin\phi_1 \sin\lambda_1 \cos\varepsilon_1 \cos\alpha_1 + \cos\phi_1 \sin\lambda_1 \sin\varepsilon_1 \\ \cos\phi_1 \cos\varepsilon_1 \cos\alpha_1 + \sin\phi_1 \sin\varepsilon_1 \end{bmatrix}_{3 \times 1} \quad (11-18)$$

$$r_{i2s}^E = \begin{bmatrix} -\sin\lambda_2 \cos\varepsilon_2 \sin\alpha_2 - \sin\phi_2 \cos\lambda_2 \cos\varepsilon_2 \cos\alpha_2 + \cos\phi_2 \cos\lambda_2 \sin\varepsilon_2 \\ \cos\lambda_2 \cos\varepsilon_2 \sin\alpha_2 - \sin\phi_2 \sin\lambda_2 \cos\varepsilon_2 \cos\alpha_2 + \cos\phi_2 \sin\lambda_2 \sin\varepsilon_2 \\ \cos\phi_2 \cos\varepsilon_2 \cos\alpha_2 + \sin\phi_2 \sin\varepsilon_2 \end{bmatrix}_{3 \times 1} \quad (11-19)$$

The direction vectors towards the satellite from the starting position at the two stations to a point beyond the satellite gives a line. When the two lines intersect this gives a point that can be taken as an a-priori value.

If X denotes the stations coordinates in ECEF system, then the starting points of the lines are the known station's coordinates and are given as:

$$A_{i1}^E = X_{i1}^E \quad (11-20)$$

$$B_{i1}^E = X_{i2}^E \quad (11-21)$$

here the superscript 'E' represents that the coordinates are in ECEF coordinate system and 'i'

represents the x, y and z coordinates.

the end points of the line can be determined as:

$$A_2^E = A_1^E + d_s \cdot r_{i_1s}^E \quad (11-22)$$

$$B_2^E = B_1^E + d_s \cdot r_{i_2s}^E \quad (11-23)$$

from these four points of the two lines the intersection of these lines can be determined as:

$$\eta_A = \left( (B_2^E - B_1^E) \times (A_1^E - B_1^E) \right) \cdot \left( (A_2^E - A_1^E) \times (B_2^E - B_1^E) \right) \quad (11-24)$$

$$\eta_B = \left( (A_2^E - A_1^E) \times (A_1^E - B_1^E) \right) \cdot \left( (A_2^E - A_1^E) \times (B_2^E - B_1^E) \right) \quad (11-25)$$

$$d_s = \left( (A_2^E - A_1^E) \times (B_2^E - B_1^E) \right) \cdot \left( (A_2^E - A_1^E) \times (B_2^E - B_1^E) \right) \quad (11-26)$$

$$A_o^E = A_1^E + \left( \frac{\eta_A}{d_s} \right) \cdot (A_2^E - A_1^E) \quad (11-27)$$

$$B_o^E = B_1^E + \left( \frac{\eta_B}{d_s} \right) \cdot (B_2^E - B_1^E) \quad (11-28)$$

The positions  $A_o$  and  $B_o$  are those two points that are closest on lines A and B. The mean value of these two points can be taken as the a-priori position for co-location satellite.

The a-priori point is determined from the first two stations at an epoch while all the stations that can see satellite at that epoch took part in coordinate determination.

As the co-location satellite is moving very fast due to low orbit so a new a-priori value is calculated again after every 5 minutes. For example the Globalstar satellite at an altitude of 1400 km above the Earth's surface orbits at a speed of 6.8 km/s. That means after every five seconds it would cover a distance of 35 km. So a new direction vectors towards the new satellite position would yield a new a-priori value.

# 12 Results & Discussion

Figure 24 presents the ground track of Globalstar satellite 37744, plotted for 1 day period with time step of 1 second. The orbital information of Globalstar satellite is given in table 1 in Chapter 1.

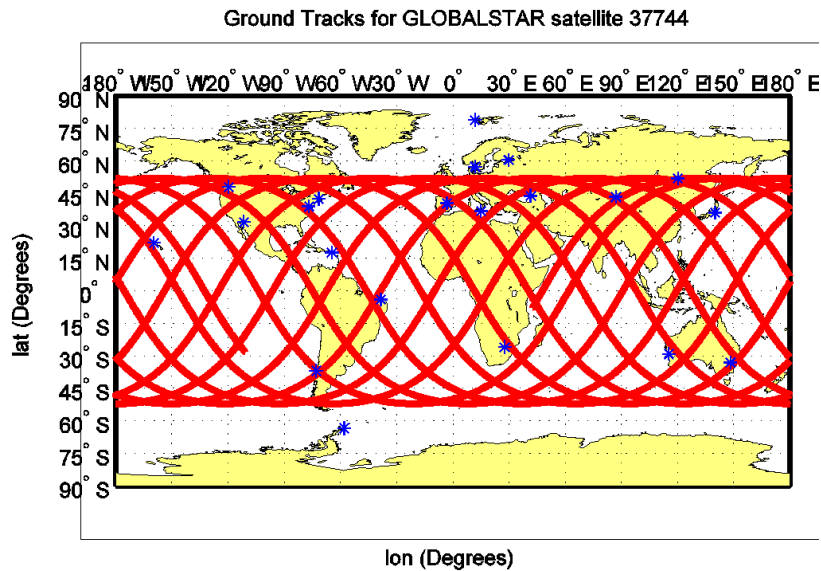


Figure 24: Ground tracks of Globalstar plotted for 1 day

The satellite's orbital inclination is  $52^\circ$  and it completes 12.6 revolutions per day. The estimated positions of Globalstar by VLBI are shown below in Figure 25.

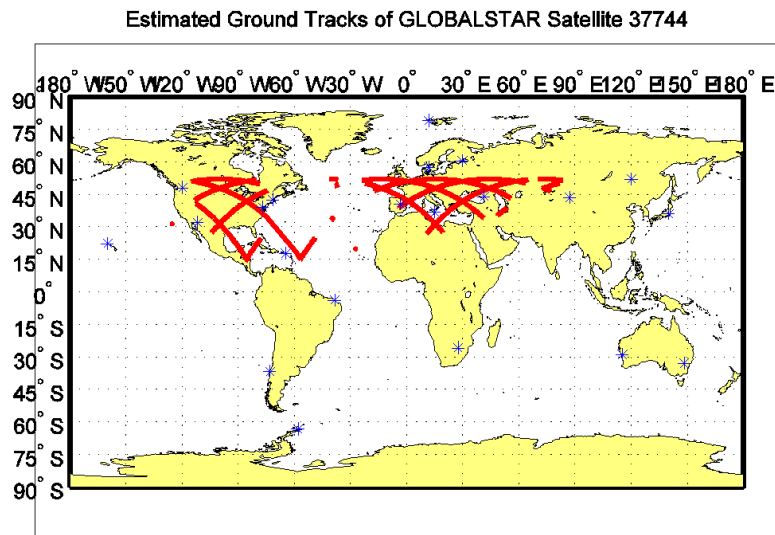


Figure 25: Estimated ground tracks of Globalstar predicted by VLBI stations

Figure 25 presents the positions of satellite estimated by the VLBI network are mostly occupied in the northern hemi-sphere. The reason is that the large numbers of our selected VLBI stations are in the northern hemisphere that satisfies the visibility condition for the four or more stations simultaneously.

There is large number of non-continuity in the estimated orbits this is due to the fact that if at some

epochs the condition for four or more stations visibility does not satisfies for a longer periods of time the positions are not estimated for those epochs.

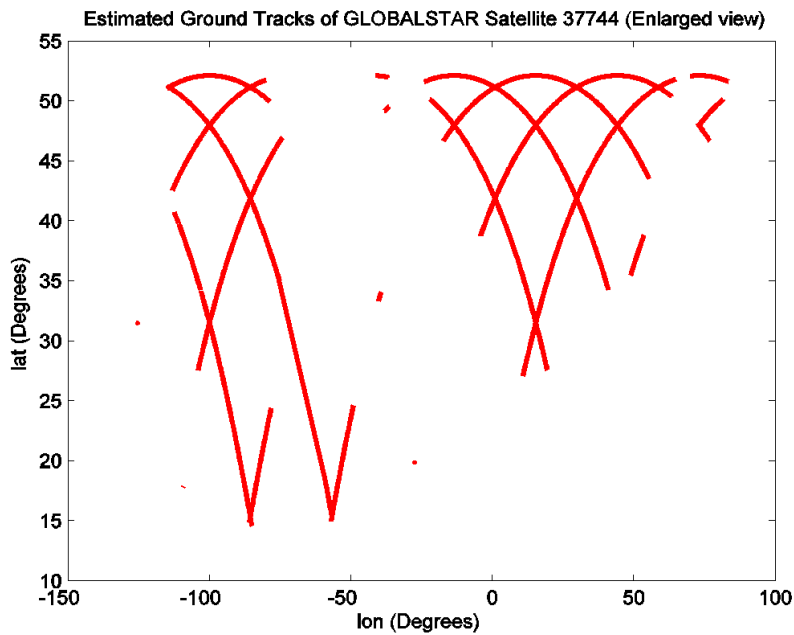


Figure 26: Enlarged view of estimated ground tracks of Globalstar estimated by VLBI

Figure 26 is the enlarged view of the estimated ground tracks for Globalstar that shows the tracks are in the northern hemisphere and the discontinuities are more visible.

The Figure 27 presents the vector difference of original and estimated positions of the colocation satellite. The plots are shown only for the epochs 7925 to 21706. The reason to plot only for this range is that 7925 is the first epoch at which four or more VLBI stations were visible to the colocation satellite. When the visibility condition is fulfilled the coordinates are determined at that epoch and for further epochs. The gap between the plotted points on the epoch axis shows that at these epochs the condition for visibility was not fulfilled and coordinates of colocation satellite were not determined.

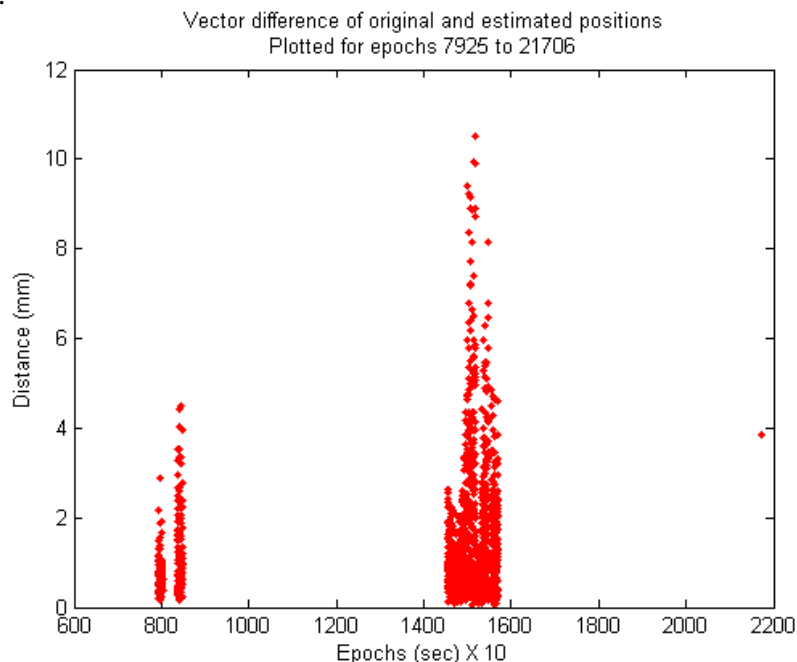


Figure 27: Vector difference of original and estimated positions of Globalstar

In total 8646 positions were estimated while only 1330 vector difference are shown in Figure 27. The reason is that there are some points that give very high values of vector difference. Those points are not shown in Figure 27. Those points fell on the epochs 21736, 70992, 71158 and 71159 and at these epochs the values of vector difference are  $5.9768e13$ ,  $1.1385e19$ ,  $4.8813e20$ ,  $2.6402e20$ , respectively, which are very unrealistic estimated positions. This is due to the fact that at these epochs the geometry of visible VLBI stations was very bad. At these epochs the least-squares estimation processes did not converged, and after 100 iterations the loop was terminated deliberately to estimate position for the next epochs.

To discard those positions with very high values of vector difference, the concept of Dilution of Precision (DOP) was implemented and only those estimated positions were selected that fell between DOP ranges 0 to 20.

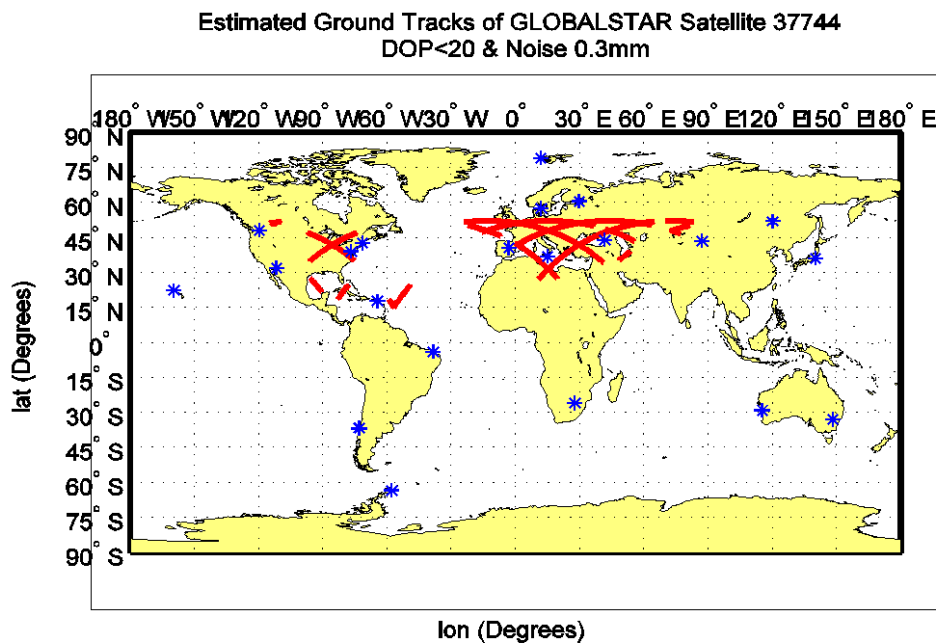


Figure 28: Estimated ground tracks DOP&lt;20 and simulated measurement noise 0.3 mm

Figure 28 shows only those estimated positions that were calculated for DOP levels less than 20. That means positions are estimated only at those epochs at which DOP is less than 20. As discussed in Chapter 9 that there are different DOP levels within the range 0-20 that provides different levels of accuracy for variety of applications and all those DOP levels with their description were summarized in the Table 7.

If the estimated positions are plotted in different colors for different levels of DOP, than it would be easier to figure out which stations are involved in estimating positions with reasonable DOP ratings. Figure 29 shows the estimated ground tracks for different DOP ranges in colors.

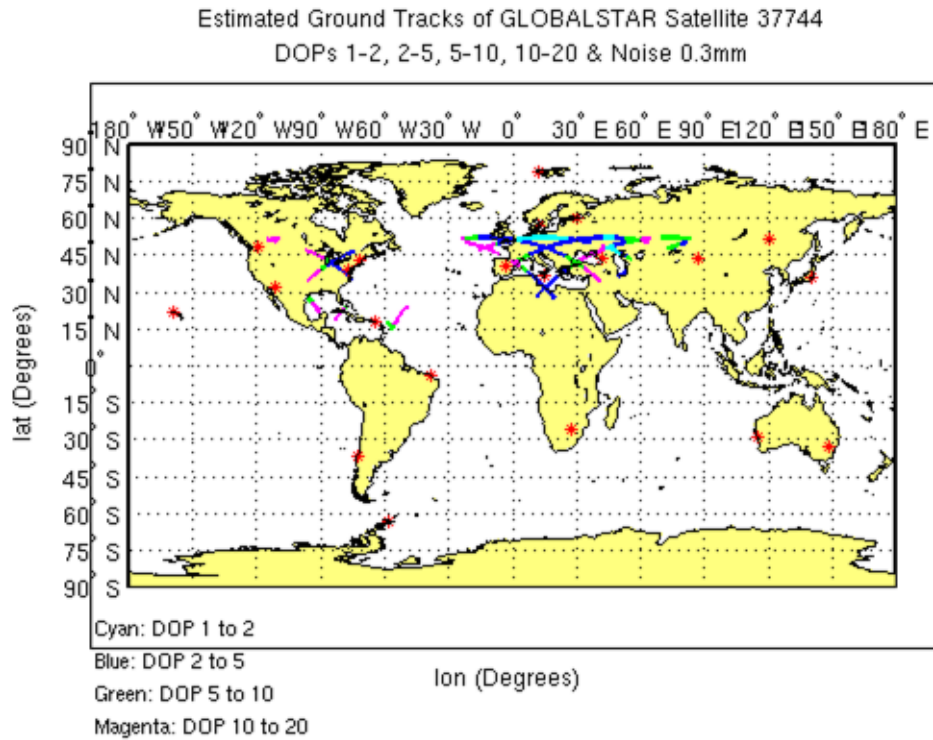


Figure 29: Estimated ground tracks colored in different DOP ranges with simulated measurement noise 0.3 mm

Figures 28 and 29 contains the same number of estimated positions but the difference is that in Figure 29 the ground tracks are colored in accordance with the DOP levels. All these estimated positions are calculated at noise levels of 0.3 mm and 1.5 mm but due to the very small difference in the positions estimated at two noise levels, only the results for 0.3 mm are shown for all the satellites. The vector difference of original and estimated positions of the satellite will tell about how much the satellite estimated positions are far from the original positions. This is shown for both the two noise levels of 0.3 mm and 1.5 mm in Figures 30 and 31 respectively.

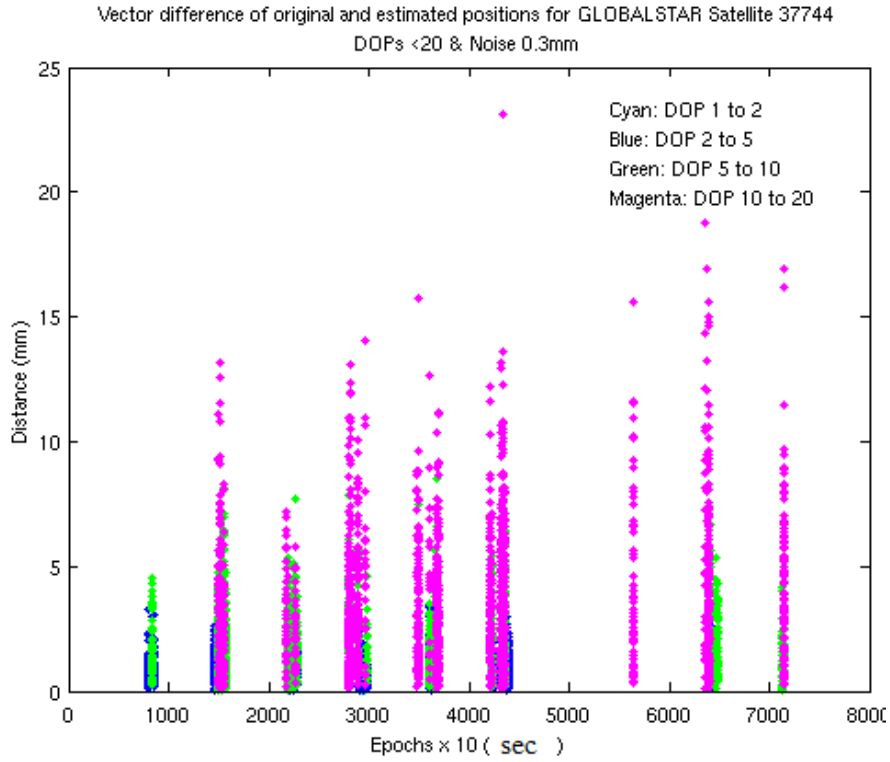


Figure 30: Vector difference for different DOP ranges and simulated measurement noise 0.3 mm

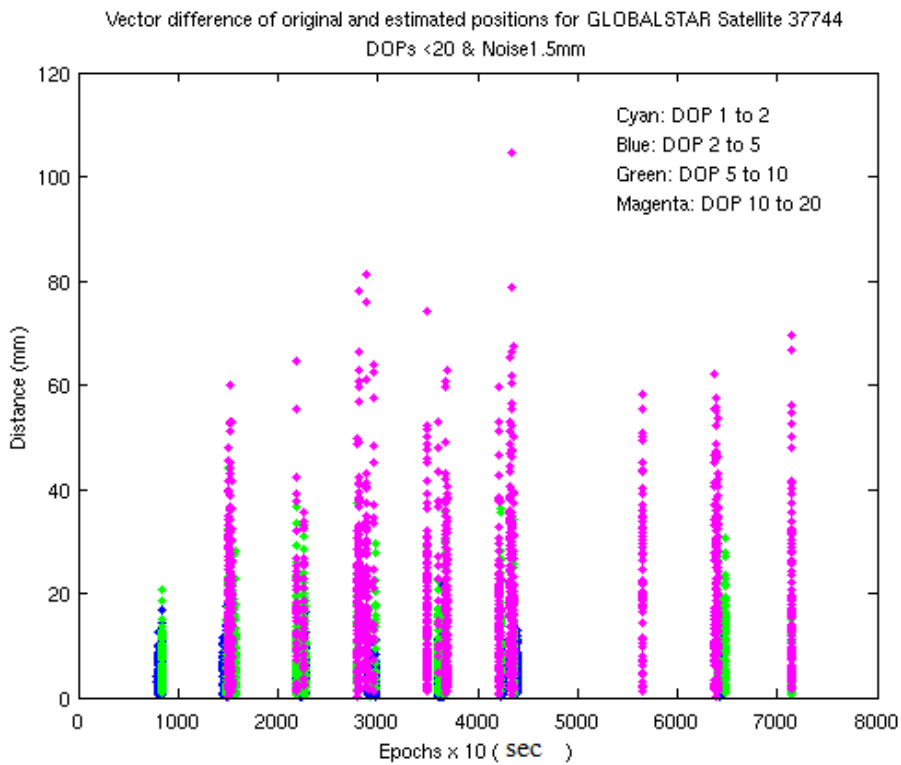


Figure 31: Vector difference for different DOP ranges and simulated measurement noise 1.5 mm

Table 9: Summary of results for Globalstar at different DOPs and simulated measurement noise levels

DOP ranges	No. of Estimated positions	DOP <sub>max</sub>	dd <sub>max</sub> mm	
			0.3 mm	1.5 mm
1-2	489	1.9997	1.8	8.3
2-5	2839	4.9997	4.0	22.0
5-10	1286	9.9994	8.5	44.0
10-20	1700	19.9910	23.1	104.6
0-20	6314	19.9910	23.1	104.6

The total number of positions estimated for Globalstar satellite are 8646. Out of these, 6314 have DOP<20. The total epochs at which the solution does not converged due to bad geometry are 4, and the non-converged epochs are 21736, 70992, 71158 and 71159. The code simulated several times for both noise levels and for each simulation the same non-converged epochs were achieved. Also the numbers of estimated positions for each DOP levels were also same but the ddmax values were slightly different, by  $\pm 1$  mm or  $\pm 2$  mm, for each noise level. The reason for this is that the noise is generated by the *randn()* Matlab function that generates normally distributed pseudo-random numbers every time the code is simulated. Changing the noise level has no effect on the number of estimated positions for each DOP level but the vector difference of original and estimated positions is affected. This can be seen in the Figures 30 and 31 and also in Table 9 that as the noise levels are increased the ddmax values also increased for each DOP level.

Figure 32 depicts the ground track of 24795 Iridium satellite, plotted for 1 day period with time step of 1 second. The orbital information of 24795 satellites is given in table 1 in Chapter 1.

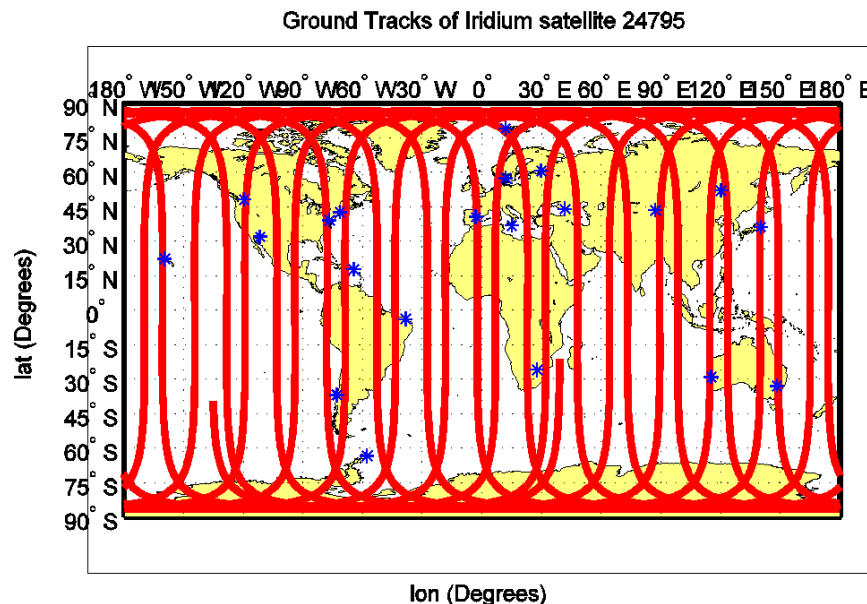


Figure 32: Ground tracks of Iridium plotted for 1 day

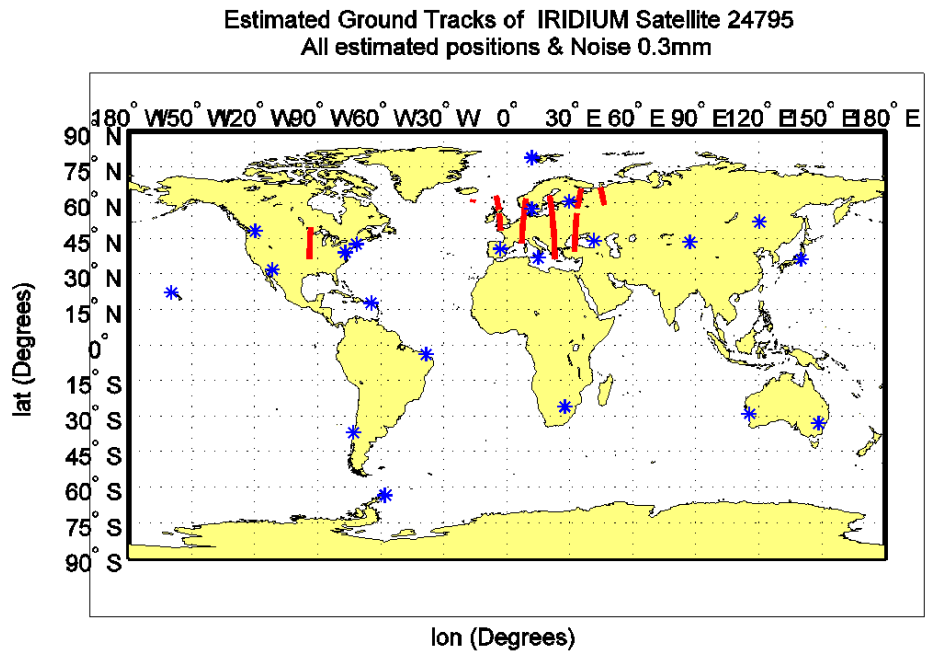


Figure 33: Estimated ground tracks of all estimated positions and simulated measurement noise 0.3 mm

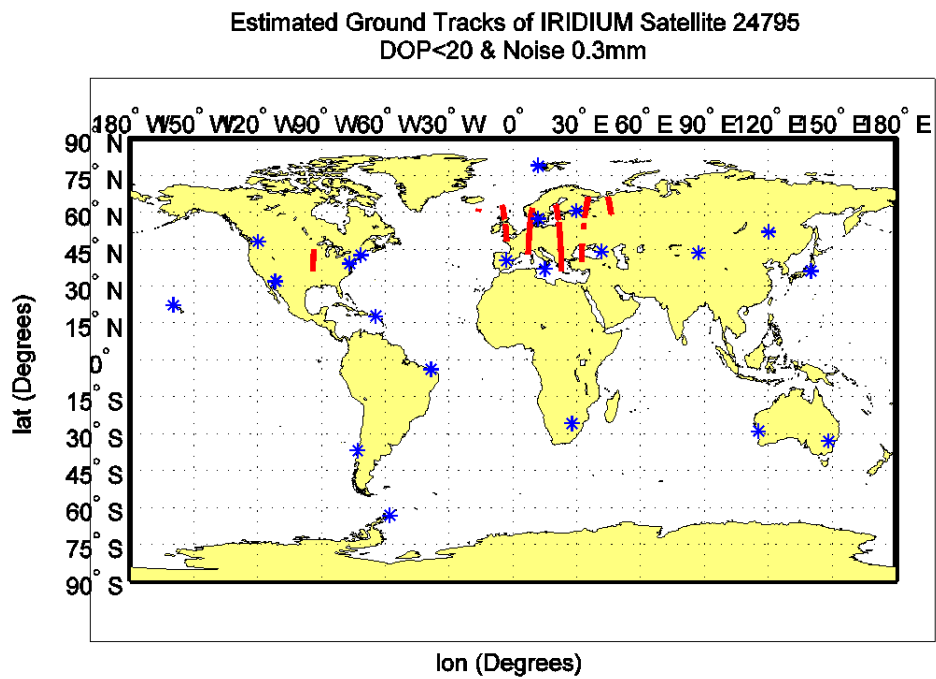


Figure 34: Estimated ground tracks DOP<20 and simulated measurement noise 0.3 mm

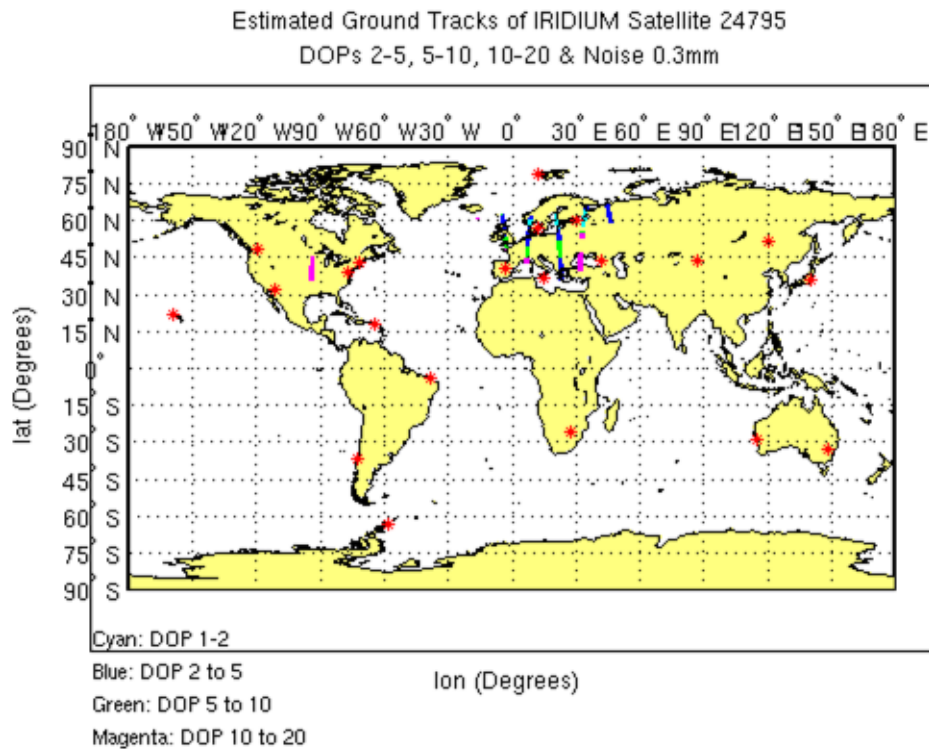


Figure 35: Estimated ground tracks colored in different DOP ranges with simulated measurement noise 0.3 mm

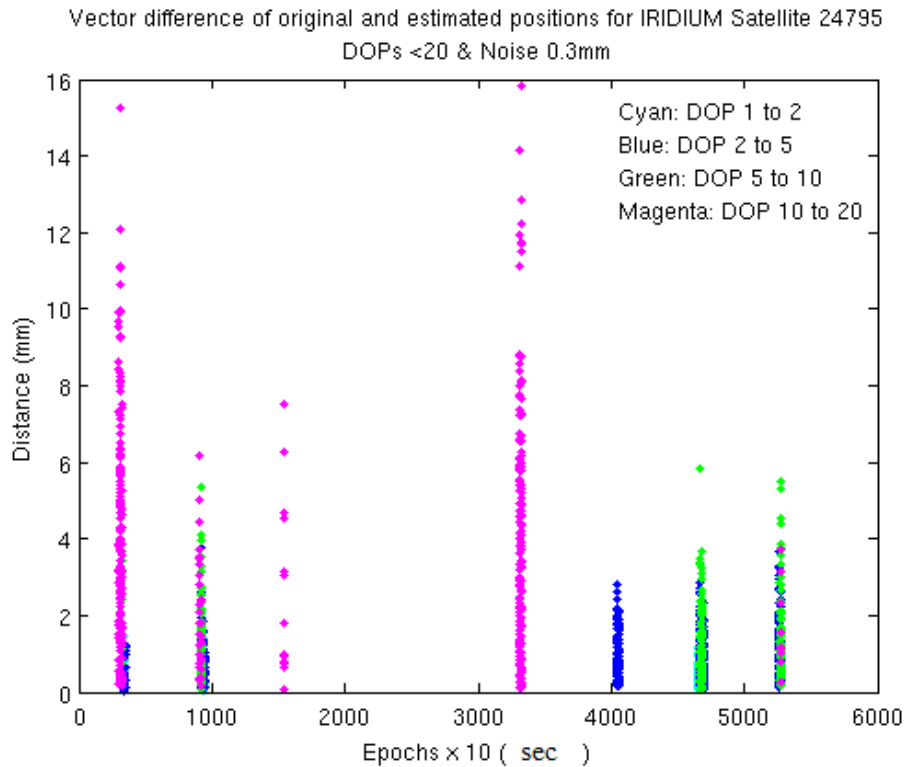


Figure 36: Vector difference for different DOP ranges and simulated measurement noise 0.3 mm

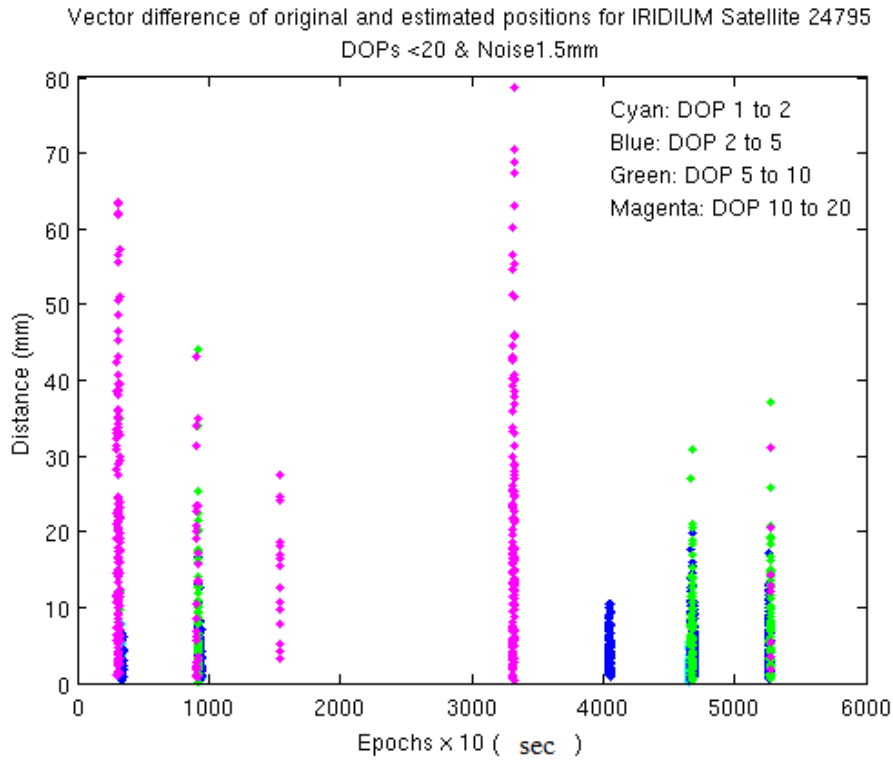


Figure 37: Vector difference for different DOP ranges and simulated measurement noise 1.5 mm

Table 10: Summary of results for Iridium at different DOPs and simulated measurement noise levels

DOP range	No. of Estimated positions	DOP <sub>max</sub>	dd <sub>max</sub> mm	
			0.3 mm	1.5 mm
1-2	277	1.98949	1.5	8.0
2-5	634	4.99442	3.8	2.0
5-10	260	9.94176	5.8	44.0
10-20	360	19.94321	15.8	78.6
0-20	1531	19.94321	15.8	78.6

In total, 1730 positions were estimated. Out of these, 1531 had DOP<20, so 199 positions were discarded. There are no epochs with non-converge values due to bad geometry.

Figure 38 depicts the ground track of Orbcomm satellite 25986, plotted for 1 day period with time step of 1 second.

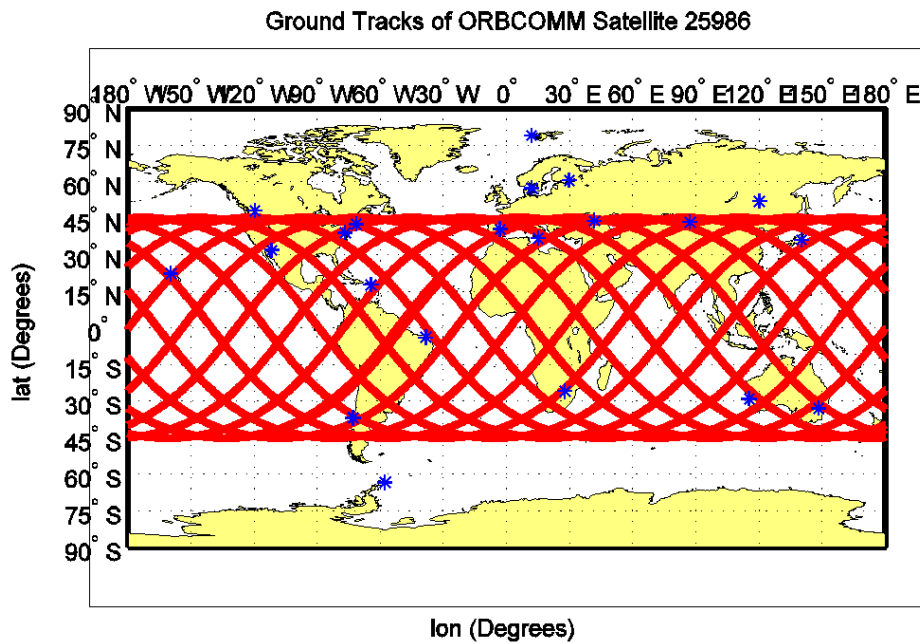


Figure 38: Ground track of Orbcomm plotted for 1 day

The ground track of Orbcomm satellite estimated by the VLBI network is shown in the figure below:

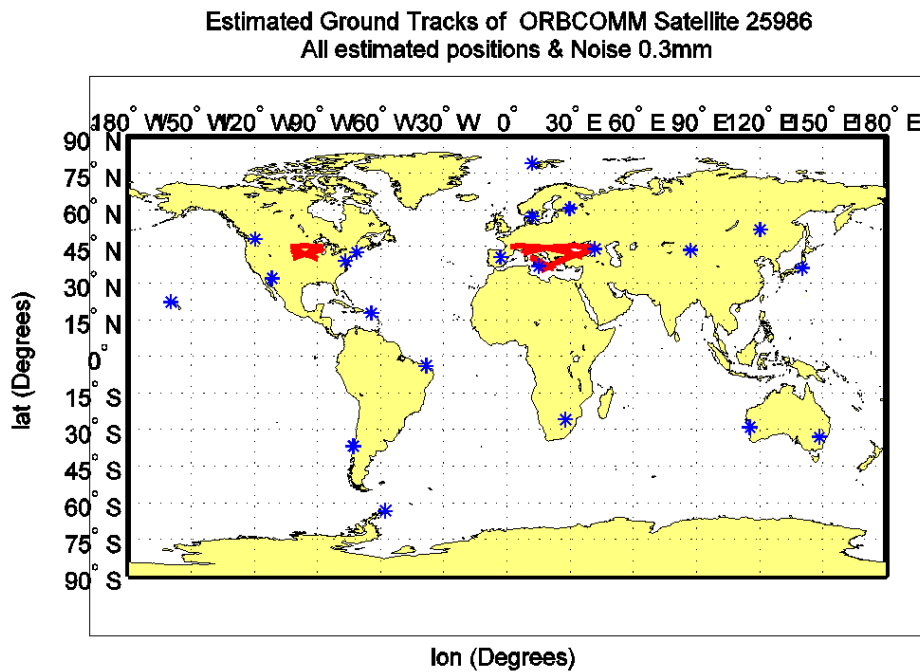


Figure 39: Estimated ground tracks of all estimated positions and simulated measurement noise 0.3 mm

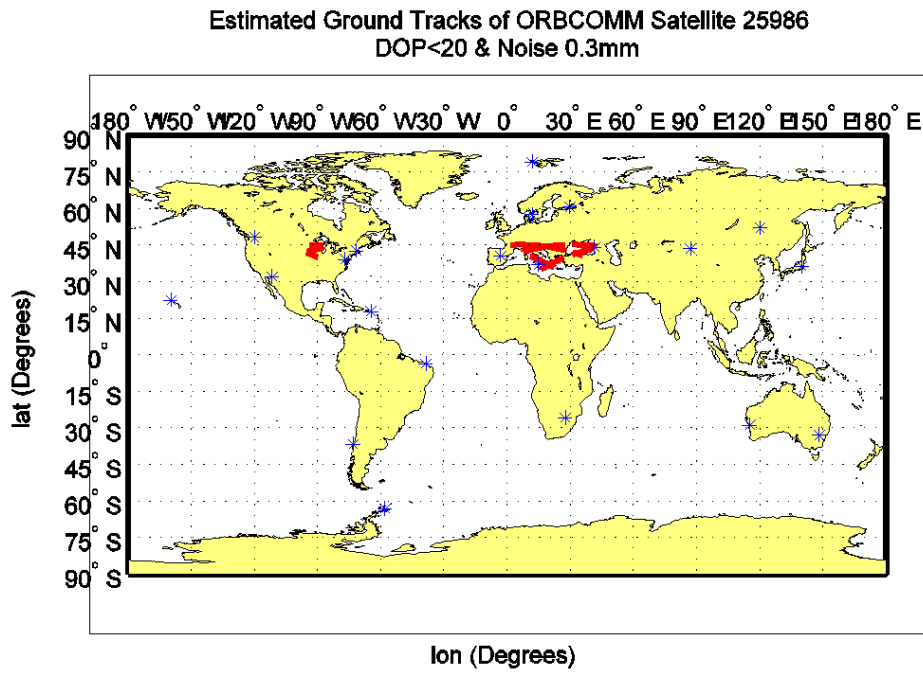


Figure 40: Estimated ground tracks DOP<20 and simulated measurement noise 0.3 mm

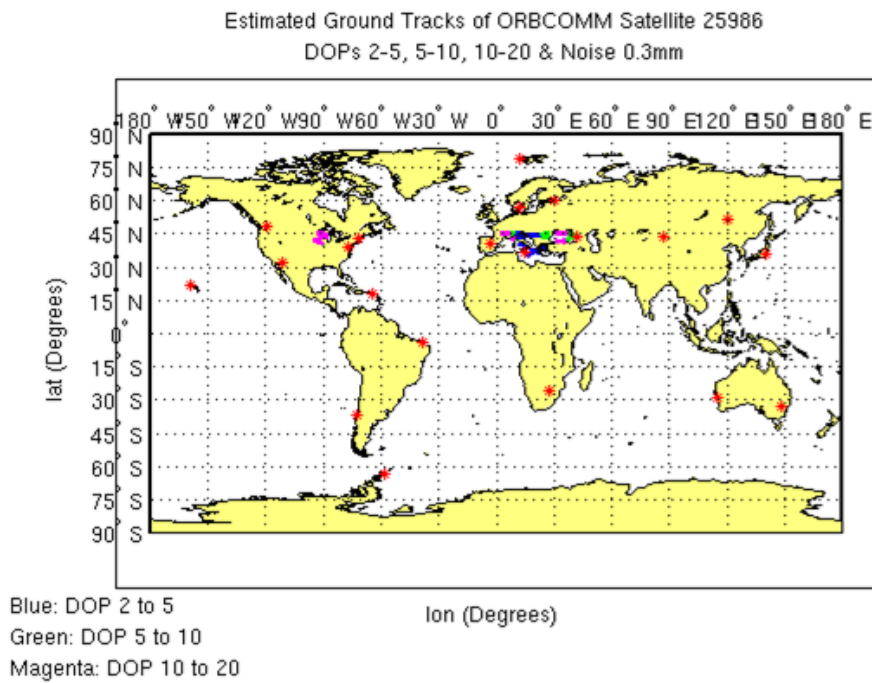


Figure 41: Estimated ground tracks colored in different DOP ranges with simulated measurement noise 0.3 mm

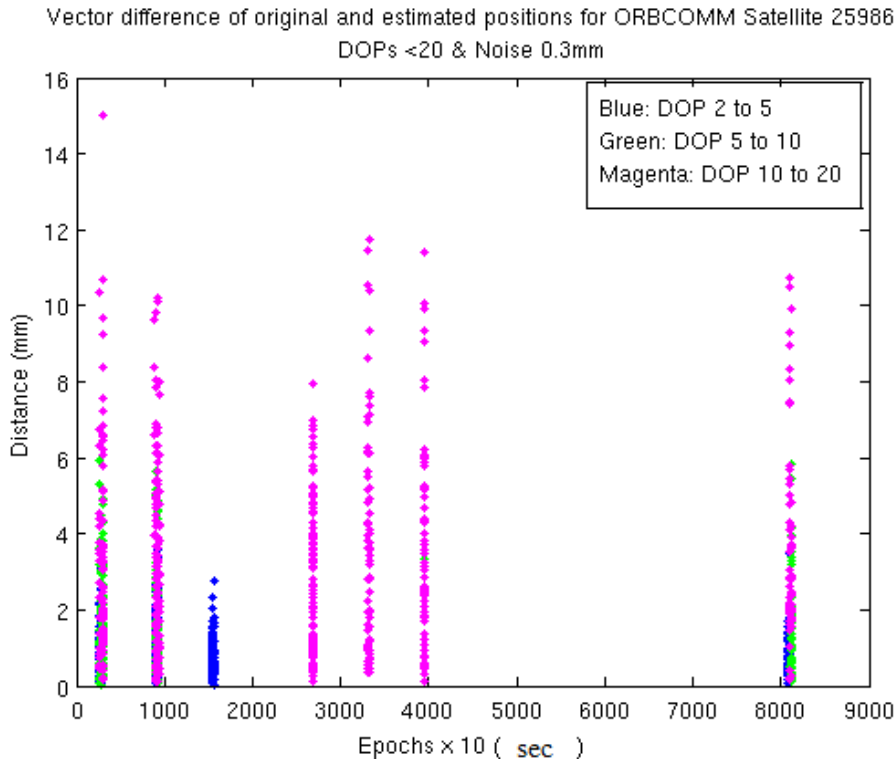


Figure 42: Vector difference for different DOP ranges and simulated measurement noise 0.3 mm

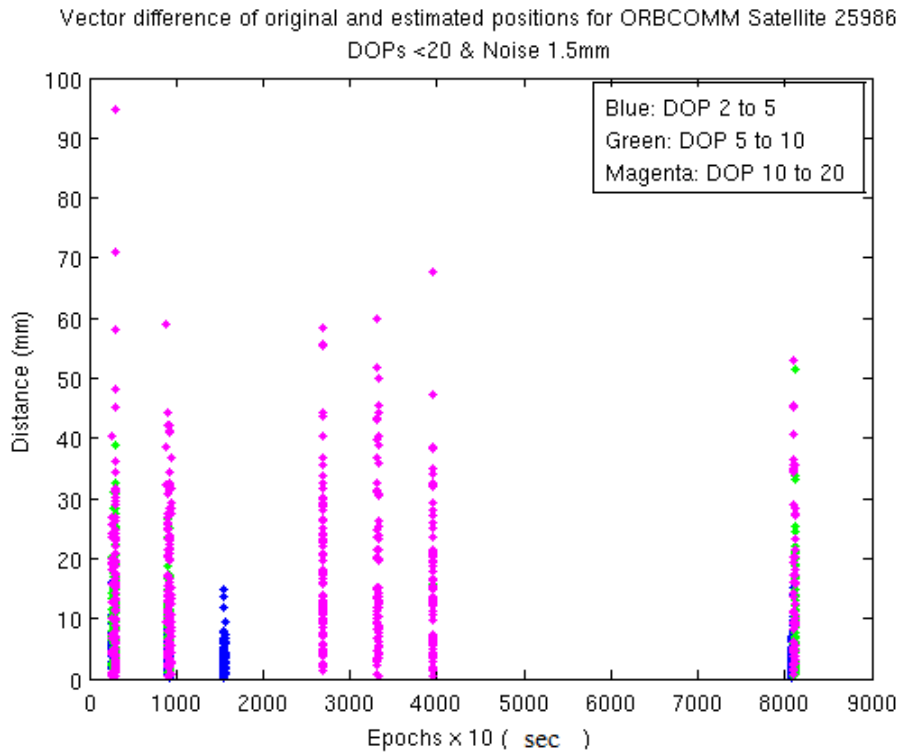


Figure 43: Vector difference for different DOP ranges and simulated measurement noise 1.5 mm

Table 11: Summary of results for Orbcomm at different DOPs and simulated measurement noise levels

DOP range	No. of Estimated positions	DOP <sub>max</sub>	dd <sub>max</sub> mm	
			0.3 mm	1.5 mm
2-5	668	4.998	4.0	17.0
5-10	282	9.989	6.0	51.5
10-20	516	19.948	15.0	94.7
0-20	1466	19.948	15.0	94.7

For Orbcomm, total positions estimated were 1958. Out of these, 1466 had DOP<20. Like Iridium there were no epochs with non-converged values due to bad geometry.

Figure 44 depicts the ground track of LAGEOS-1 satellite, plotted for 1 day period with time step of 1 second. The orbital information of LAGEOS-1 satellite is given in table 1 in Chapter 1.

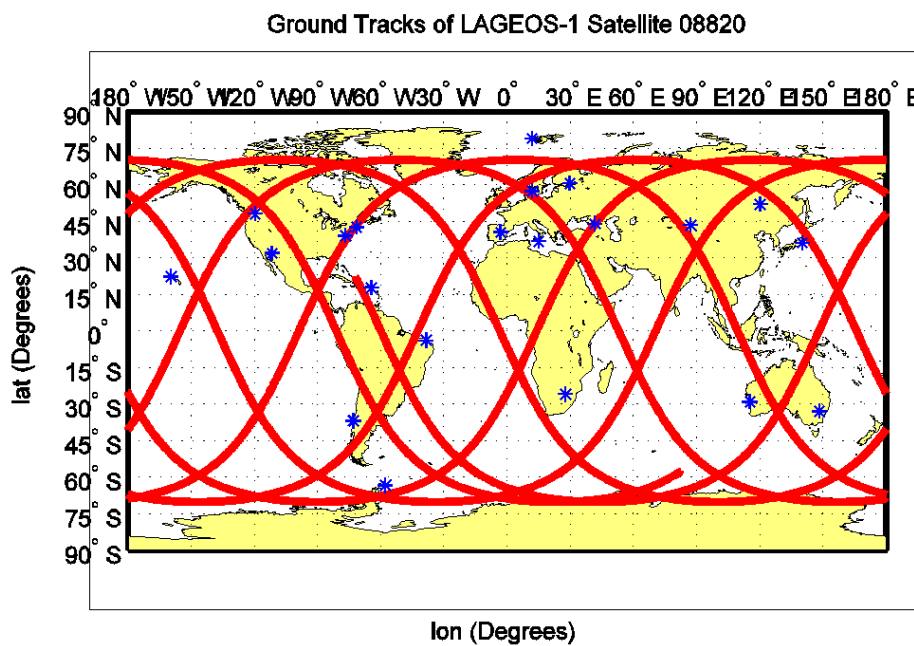


Figure 44: Ground track of LAGEOS-1 plotted for 1 day

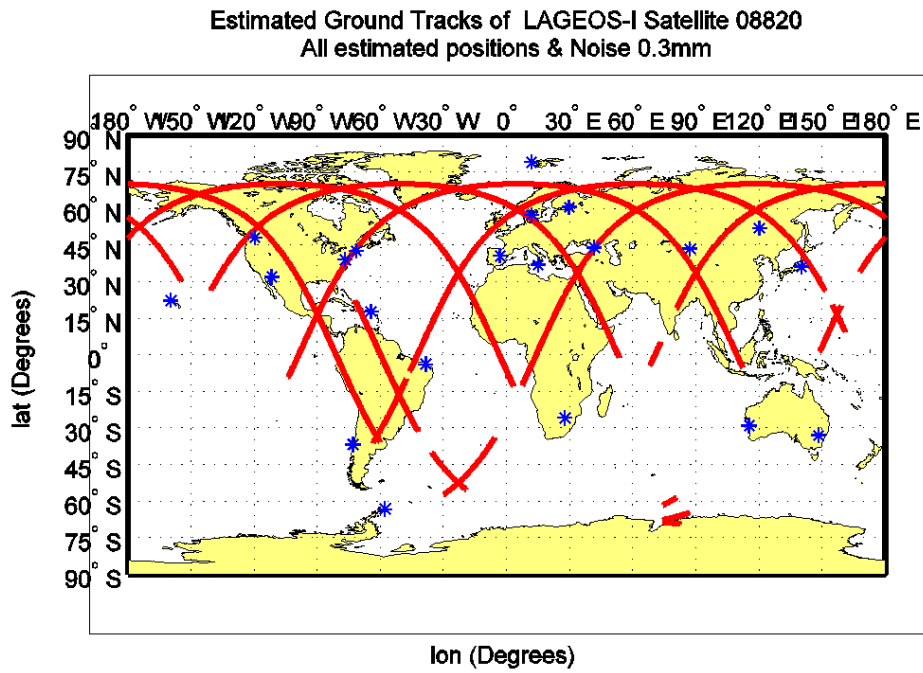


Figure 45: Estimated ground tracks of all estimated positions and simulated measurement noise 0.3 mm

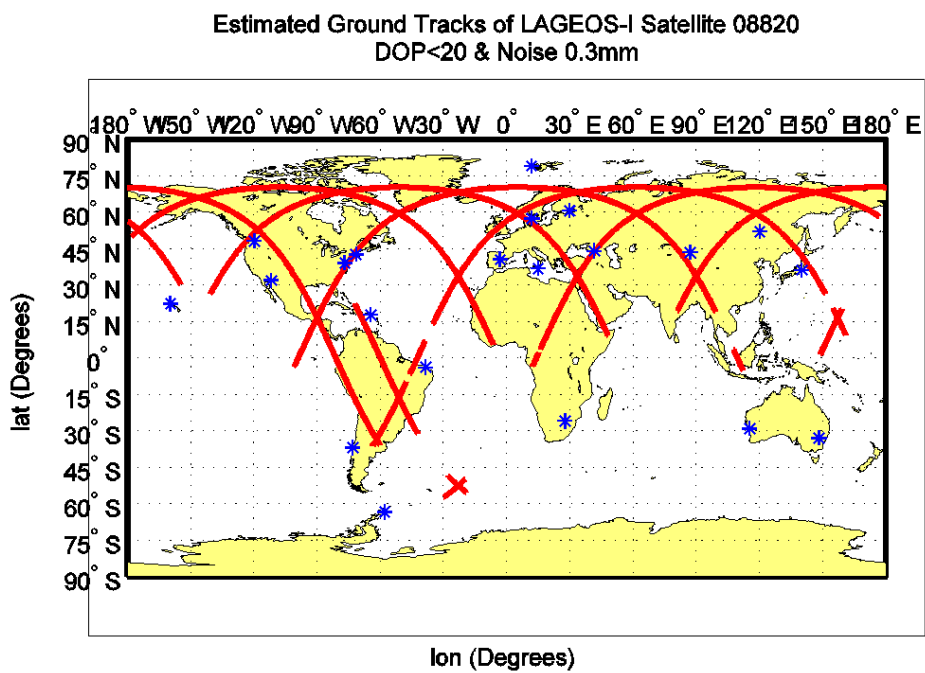


Figure 46: Estimated ground tracks DOP < 20 and simulated measurement noise 0.3 mm

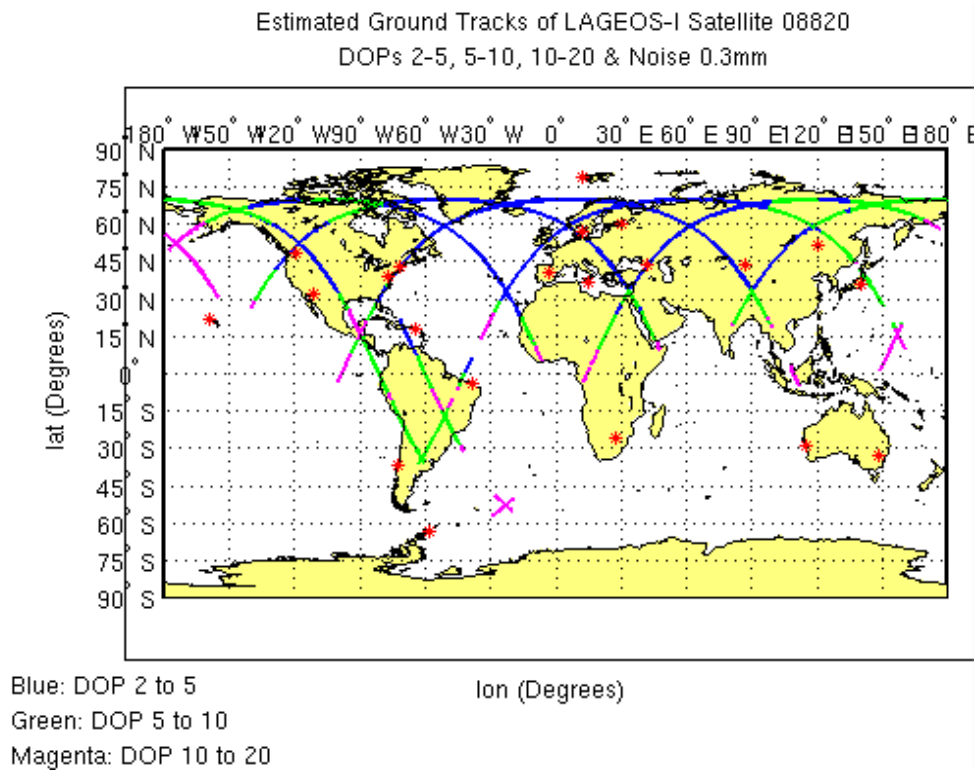


Figure 47: Estimated ground tracks colored in different DOP ranges with simulated measurement noise 0.3 mm

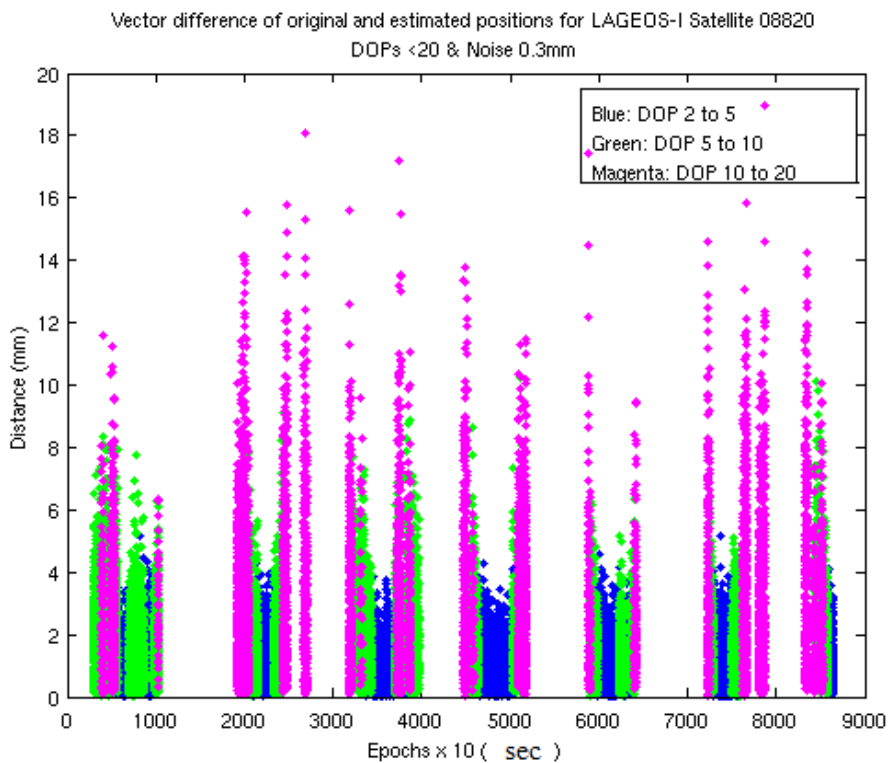


Figure 48: Vector difference for different DOP ranges and simulated measurement noise 0.3mm

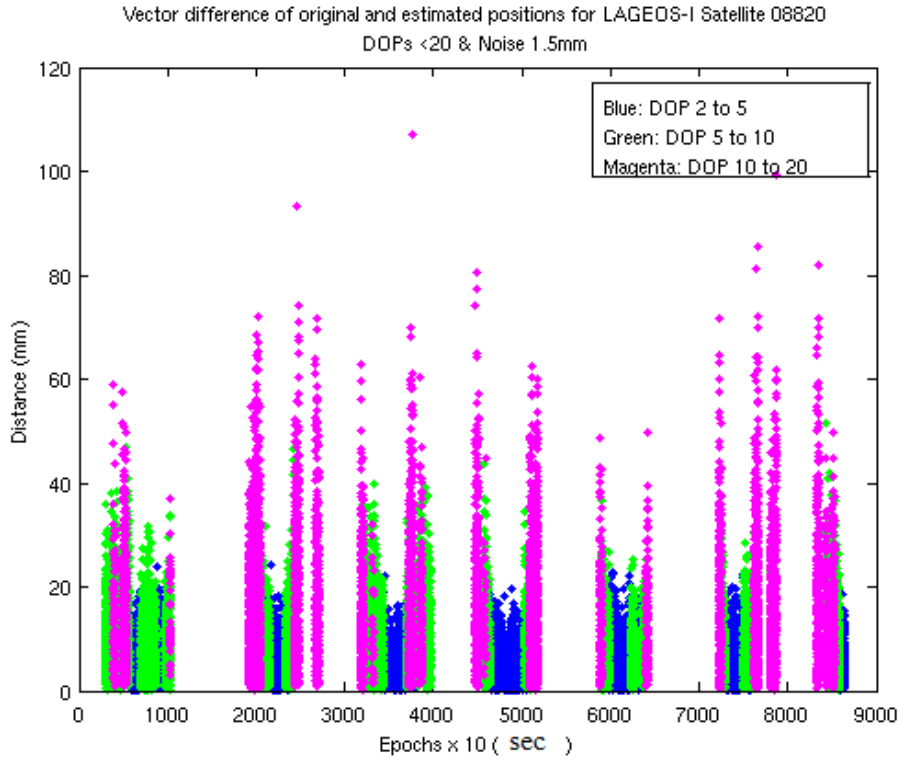


Figure 49: Vector difference for different DOP ranges and simulated measurement noise 1.5mm

Table 12: Summary of results for LAGEOS-1 at different DOPs and simulated measurement noise levels

DOP range	No. of Estimated positions	DOP <sub>max</sub>	dd <sub>max</sub> mm	
			0.3 mm	1.5 mm
2-5	18423	4.999	5.2	24.0
5-10	14442	9.999	10.2	51.6
10-20	7096	19.999	19.0	107.2
0-20	39961	19.999	19.0	107.2

In total 45359 positions estimated. Out of these, 39961 had DOP<20. There is only one epoch at which the solution did not converge due to bad geometry and the non-converged Epoch is 71724. The LAGEOS-1 satellite presented the highest number of estimated positions and that is due the higher altitude compared to other tested satellites.

## 13 Conclusion

The results for all the tested satellites leads to the conclusion that the satellites at higher altitudes, above the Earth's surface, of 6000 km or more will lead to the better tracking by the selected VLBI stations and GNSS satellites. If only the GNSS case is taken into account, even the lower altitudes of 800 km will provide good predictions of the satellite positions as there are 30 GNSS satellites selected in the network. Also the vector difference of original and estimated positions was of the order of mm, with 1 mm deliberately added measurement noise, for the acting co-location satellites. But as the co-location satellite has to be equipped with VLBI instruments also, so the lower altitudes will not provide tracking for the longer periods of time unless the numbers of VLBI stations are increased. There are total thirty one VLBI stations listed on the 'International VLBI Service for Geodesy & Astrometry' website but only twenty one stations are selected in this project. If the numbers of stations are increased to thirty one, the estimated positions for LEO satellites are also likely to be increased by a considerable amount. But only positions in the northern hemisphere are likely to be increased as large part of listed VLBI stations are in the northern hemisphere.

The orbital height of Iridium and Orbcomm is almost the same, averaging almost 800 km but the inclinations are  $86^\circ$  and  $45^\circ$  respectively. The Iridium even with the higher inclination angle did not produced the large number of estimated positions. The total estimated positions were 1730, only 2% of the day, while total estimated positions for Orbcomm were 1958, only 2.27% of the day, which shows that inclination did not affected the estimations as much.

The Globalstar satellite has inclination of  $52^\circ$  and orbital height of 1400 km. So the positions estimated by VLBI were 10% of the day which is comparatively higher with the Iridium and Orbcomm respectively, and that is mostly due to the increased orbital height.

LAGEOS satellite at an altitude of 6000 km produced good results compared to LEO satellites. Total positions estimated were 45359 i.e. 52.5% of the day. 18423 positions had DOP levels in the range 2-5 which is rated as 'Good' for reliable estimations. The inclination of 08820 is  $109^\circ$  which enables motion of the satellite in the direction opposite to the Earth's rotation i.e. a retrograde orbit, but considering the above discussion for LEO satellites, it does not seems to be influential on the estimation process.

The elliptical orbits are useful for communication satellites where communication services are needed in a specific region for longer periods of time. As the co-location satellite have to be tracked by the VLBI stations all over the world so elliptical orbit is not a good choice. Many remote sensing and geodetic satellites are in LEO, circular orbits to provide equal proportion of visibility to existing ground tracking stations. So circular orbits with altitudes of 6000 km or more are a good choice for co-location satellite. At these heights the measure should also be taken to protect satellite from 'Van Allen radiation belt' and appropriate shielding should be provided. The sun-synchronous orbits are useful to provide continuous sunlight to the solar-panels of co-location satellite and save the battery life time.

# References

- [1] Geodetic reference antenna in space (grasp) – a mission to enhance space-based geodesy. Yoaz Bar-Sever, Bruce Haines, Willy Bertiger, Shailen Desai, Sien Wu.
- [2] Reference Frames: Determination and Interconnections, J. O. Dickey, J.L Fanselow, W.G. Melbourne, XX Newhall, E.M Standish and J.G. Williams. JPL, California Institute of Technology, Pasadena, USA
- [3] [http://www.iers.org/nn\\_10404/IERS/EN/Science/Techniques/doris.html](http://www.iers.org/nn_10404/IERS/EN/Science/Techniques/doris.html)
- [4] Fundamentals of Astrodynamics and Applications, [D.A. Vallado](#)
- [5] <https://reuscats.wikispaces.com/Coordinate+Systems>
- [6] *Orbital Mechanics with Numerit*, <http://www.cdeagle.com/omnum/pdf/csystems.pdf>
- [7] Revisiting Spacetrack Report #3, David A. Vallado , Paul Crawford , T. S. Kelso.
- [8] <http://celestrak.com/columns/v04n03/>
- [9] [http://www.castor2.ca/03\\_Mechanics/03\\_TLE/](http://www.castor2.ca/03_Mechanics/03_TLE/)
- [10] [http://en.wikipedia.org/wiki/Simplified\\_perturbations\\_models](http://en.wikipedia.org/wiki/Simplified_perturbations_models).
- [11] SPACETRACK REPORT NO. 3 , Models for Propagation of NORAD Element Sets, Felix R. Hoots, Ronald L. Roehrich, December 1980, Package Compiled by TS Kelso, 31 December 1988
- [12] Miura, Nicholas Zwiap (2009). "[Comparison and design of simplified general perturbation models](#)". *California Polytechnic State University, San Luis Obispo*.
- [13] Vallado, David A. "[Revisiting STR#3](#)". *AIAA/AAS Astrodynamics Specialist Conference, August 2006*. American Institute of Aeronautics and Astronautics.
- [14] [www.faa.gov/about/office\\_org/headquarters\\_offices/ato/service\\_units/techops/navservices/gnss/faq/gps/#8](http://www.faa.gov/about/office_org/headquarters_offices/ato/service_units/techops/navservices/gnss/faq/gps/#8)
- [15] *ERR061- Satellites in Communications and Navigation 2004/2005*, Homework 6-A, the suggested solution, Department of Radio and Space Science, Chalmers University of Technology.
- [16] *Basics of the GPS Techniques: Observation Equations*, Geoffrey Blewitt, Department of Geomatics, University of Newcastle, Newcastle upon Tyne, NE1 7RU, United Kingdom.
- [17] <http://www.amsat.org/amsat/keps/formats.html>
- [18] [www.wikipedia.org/wiki/Dilution\\_of\\_precision\\_\(GPS\)](http://www.wikipedia.org/wiki/Dilution_of_precision_(GPS))
- [19] VLBI for Space Applications, Herald Schuh, Lucia Plank, Caroline Schonberger, Johannes

Bohm, Unified Analysis Workshop, sept 16-17, 2011, Zurich CH.

[20] 'Computing NORAD mean orbital elements from a state vector, Thesis, CDO Dwight E. Andersen, B.S. Captain. USAF.

[21] Light-Time Solution, Section 8, Formulation for Observed and Computed Values of Deep Space Network Data Types for Navigation, Theodore D. Moyer, MONOGRAPH 2, DEEP SPACE COMMUNICATIONS AND NAVIGATION SERIES, Jet Propulsion Laboratory, California Institute of Technology.

[22] <http://www.souterrain.biz>

[23] Modelling Very Long Baseline Interferometry (VLBI) observations, Kamil Teke, Emine Tanır Kayıkç, Johannes Böhm and Harald Schuh, Journal of Geodesy and Geoinformation, Vol.1, No.1 pp. 17 - 26, May 2012.

[24] Orbital Mechanics, 3rd Edition, Vladimir A. , Chobotov, AIAA Education series.

[25] [www.heavens-above.com](http://www.heavens-above.com)

[26] Master thesis proposal, titled 'Simulations of a satellite system for co-location in space'

--- The picture on the title page of the GPS satellite constellation around the Earth is taken from the website <http://orbiterchspacenews.blogspot.se/> .